Supplementary Information

Innovative Design of Fluorescent PLGA – 1,8-Naphthalimide Nanoparticles as Multifunctional Materials for Next-Generation Nanotechnology and Biomedicine

Yuriev Danil,[a] Tkachenko Sergey,[a] Ermolin Danila,[b] Ivanov Ilya,[b] Melnikov Pavel,[c] Malinovskaya Julia,[a] Ryabova Anastasia,[d e f] Mishin Alexander,[g] Perfilov Maxim,[g] Ramil Khasbiullin,[h] Medvedev Mikhail,[b] Skorb Ekaterina,[b] Oshchepkov Maxim,[a] Gelperina Svetlana [a] and Oshchepkov Alexander[i,j]*

a. Mendeleev University of Chemical Technology of Russia, Miusskaya pl., 9, Moscow, 125047, Russian Federation.
b. Infochemistry Scientific Center, ITMO University, 9 Lomonosova Str., St. Petersburg, 191002, Russian Federation.
c. Rudolf Virchow Center, Center for Integrative and Translational Bioimaging, University of Wuerzburg, Josef-Schneider-Str. 2, Würzburgб, 97080, Germany
d. Prokhorov General Physics Institute of the Russian Academy of Sciences, Vavilov Str. 38, Moscow, 119991, Russian Federation.
e. National research nuclear university MEPHI, Kashirskoye Highway 31, Moscow, 115409, Russian Federation.
f. RUDN University, Miklukho-Maklaya str. 6, 117198, Moscow, Russian Federation.
g. Shemyakin-Ovchinnikov Institute of Bioorganic Chemistry, RAS (IBCh RAS), Miklukho-Maklaya 16/10, Moscow, 117997, Russian Federation.
h. Frumkin Institute of Physical Chemistry and Electrochemistry Russian Academy of Sciences (IPCE RAS), 31-4, Leninsky prospect, Moscow, 119071, Russian Federation.
i. Martin Luther University Halle-Wittenberg, Kurt-Mothes-Straße 2, D-06120 Halle, Germany.
j. Max Planck Institute for the Science of Light, Department of Physics, d-91058 Erlangen, Germany

E-mail: aleksandr.oshchepkov@chemie.uni-halle.de

Table of contents

Table S1. Comparative table of spectral properties of fluorophores in free form, as part of PLGA nanoparticles and quantum dot (QD)-loaded PLGA nanostructure

Fluorophore	λ^{abs}, nm	λ^{fl}, nm	**QY, %**	**ε,** $\frac{L}{mol \times cm}$	**QY in NP, %**	**Medium**	**Ref.**
Encapsulation of dye in PLGA nanoparticles							
Indocyanine green	785	815	2.7	262 100	6.6	PBS	[1]
Rh 123	512	531	90	85 200	46.8	EtOH	[2]
DiI	549	565	7.0	148 000	14.91	DDW/PBS Methanol	[2]
Coumarin 6	460	500	78	54 000	91.9	Ethanol	[2]
TPETPAFN	510	750	52.5	91 600	34	DDW	[3]
Covalently modified PLGA nanoparticles							
Cy3	548	561	4	150 000	73.34	PBS	[4]
Cy5	658	677	40	250 000	44.5	Ethanol	[2]
Cy5.5	683	703	27	250 000	50	H_2O/PBS	[2]
BODIPY FL	502	511	90	80 000	90	MeOH	[5]
DY-700	700	725	~ 20	140 000	not specified	PBS	[6] [7]
Quantum Dot-Loaded PLGA nanoparticles							
CdTe/CdSe	570	760	52	–	50	Chloroform	[8]
CdSe/ZnS	405	610	~26	–	~42	PBS	[9]
TOPO-CdSe/ZnS	475	514	50	–	50	Ethanol	[10]

1. Confirmation of the structure of PLGA-1,8-naphthalimide conjugates.

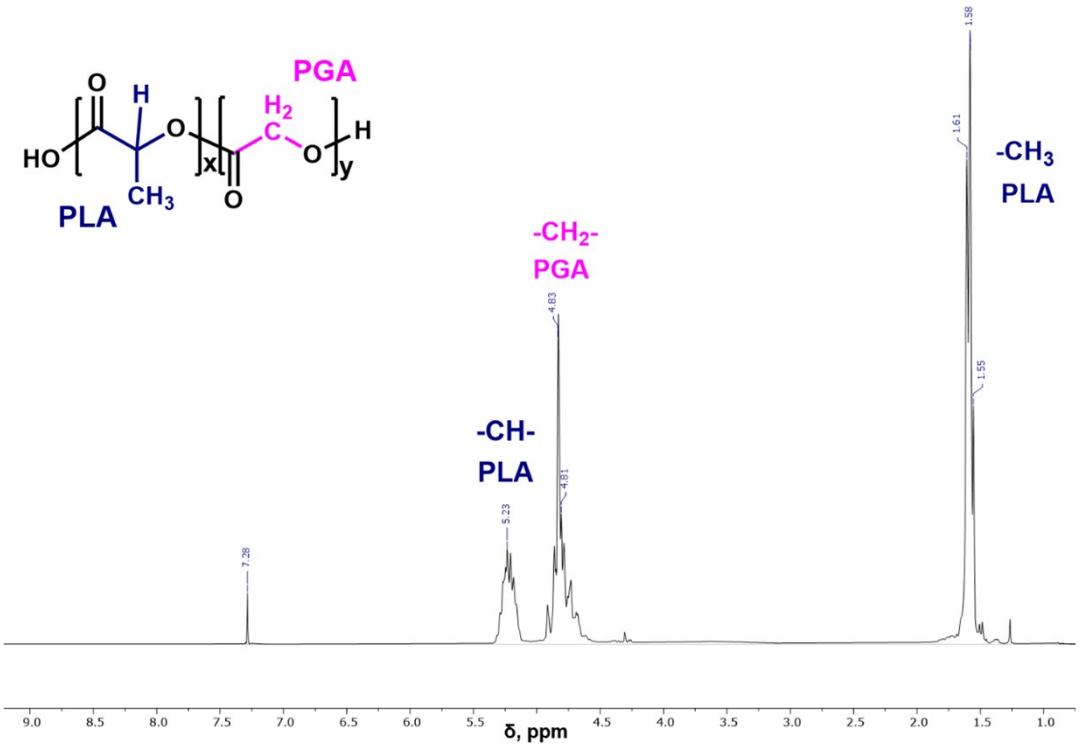

Figure S1. ^{1}H NMR spectrum of PLGA in $CDCl_3$.

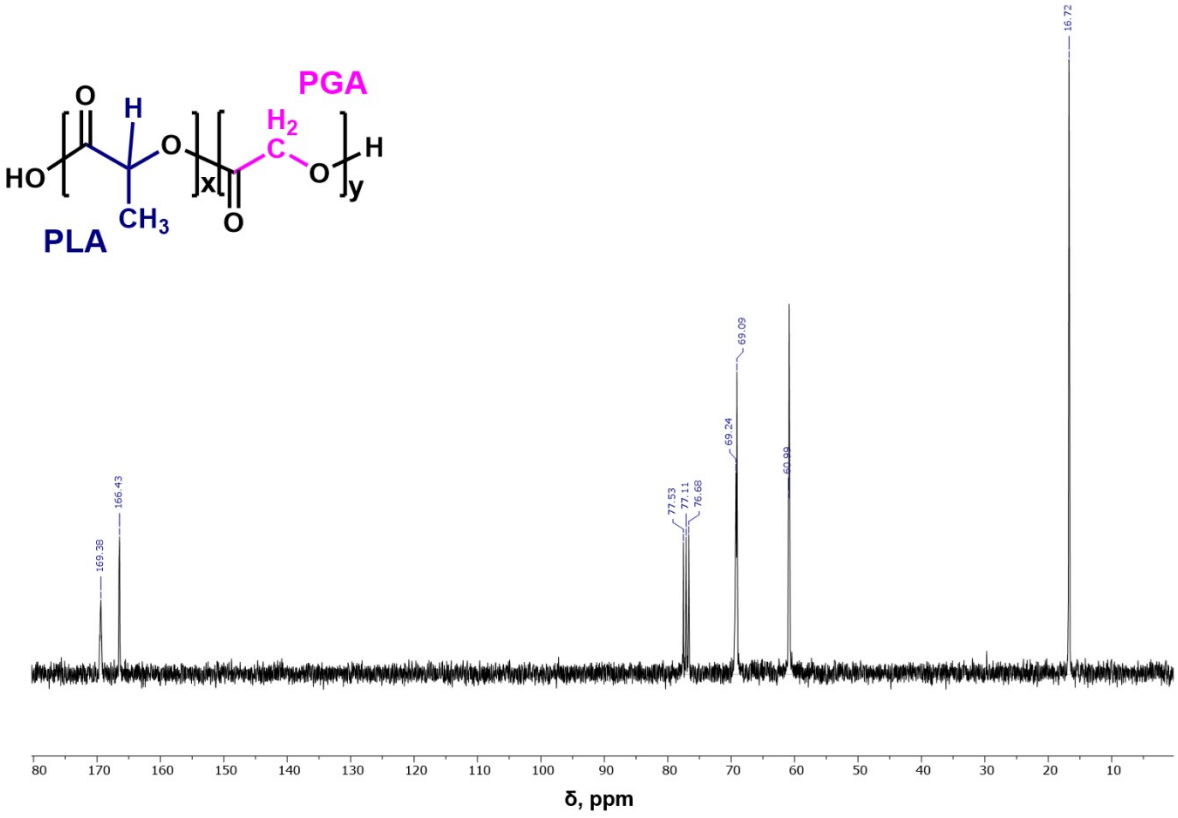

Figure S2. ^{13}C NMR spectrum of PLGA in $CDCl_3$.

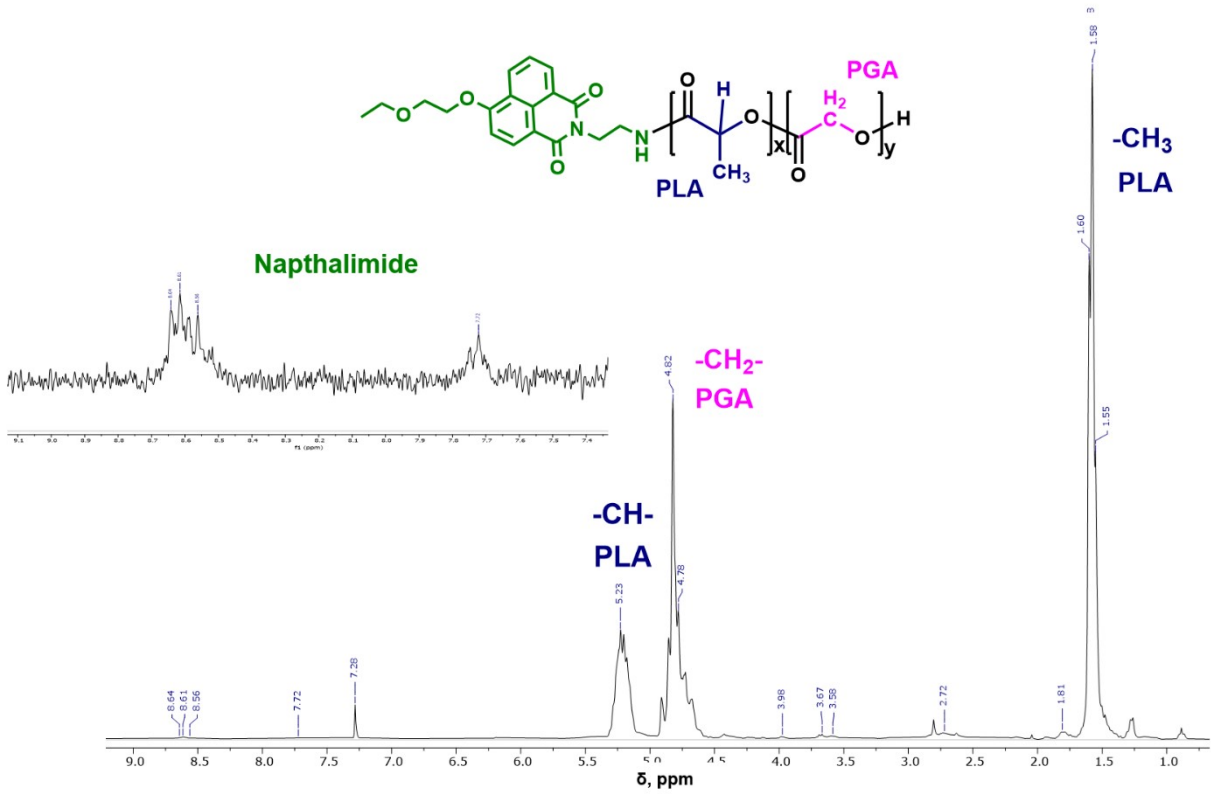

Figure S3. ^{1}H NMR spectrum of conjugate PLGA-**5** in $CDCl_3$.

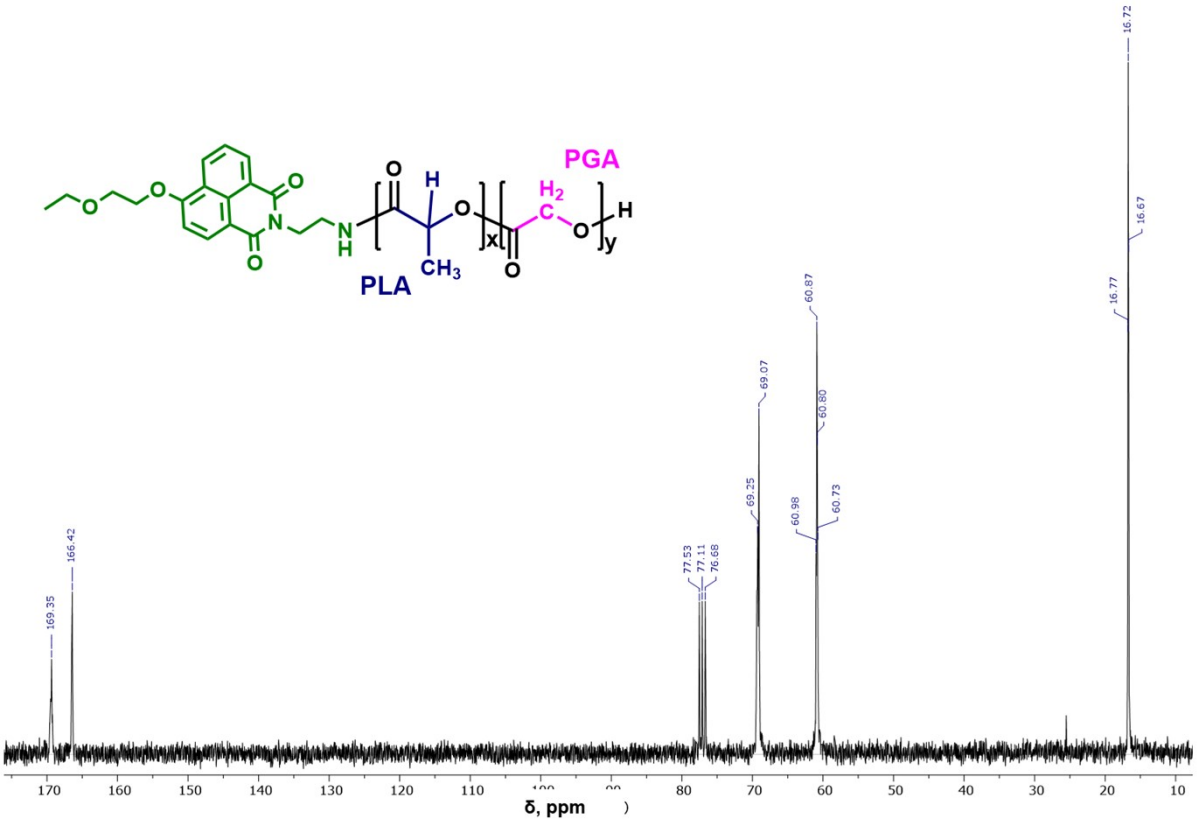

Figure S4. ^{13}C NMR spectrum of conjugate PLGA-**5** in $CDCl_3$.

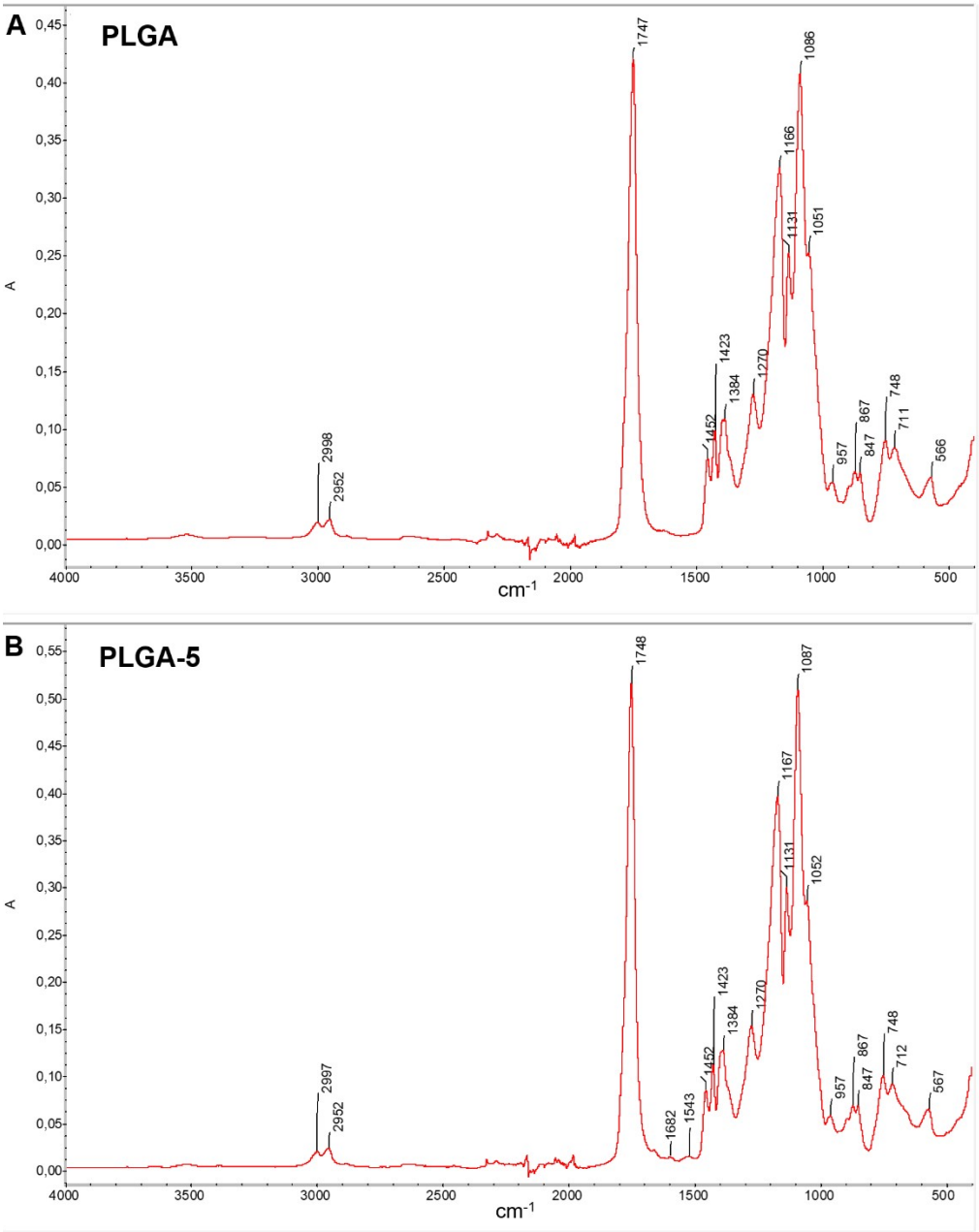

Figure S5. A) IR spectrum of unmodified PLGA; B) IR spectrum of the PLGA-**5** conjugate.

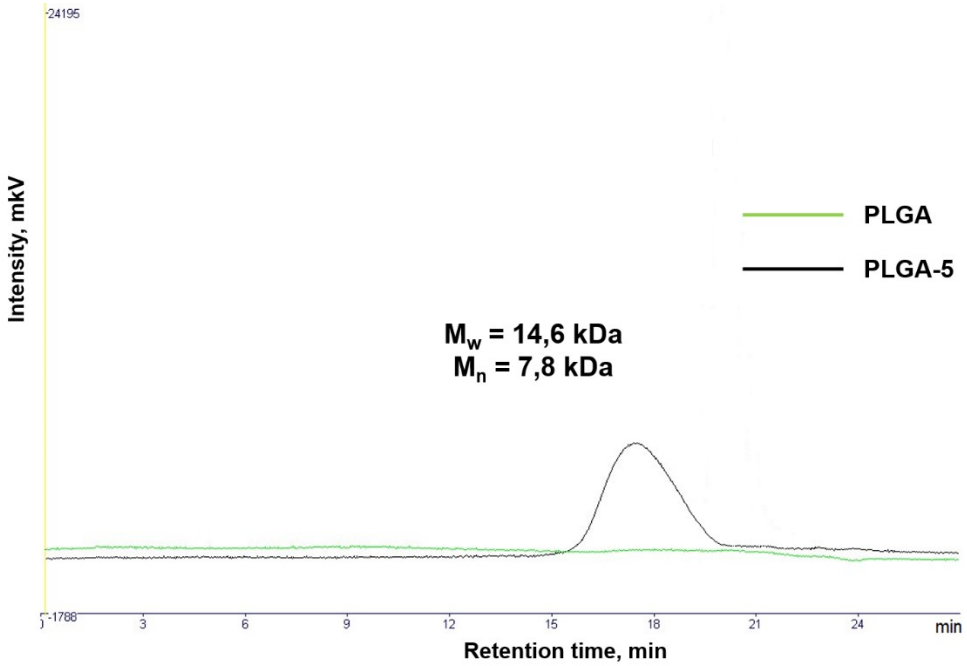

Figure S6. Gel-permeation chromatogram of PLGA-**5** conjugate. Green – unmodified PLGA polymer. Black – modified PLGA-5 polymer. (M_w: mean molecular weight; M_n: number-average molecular weight).

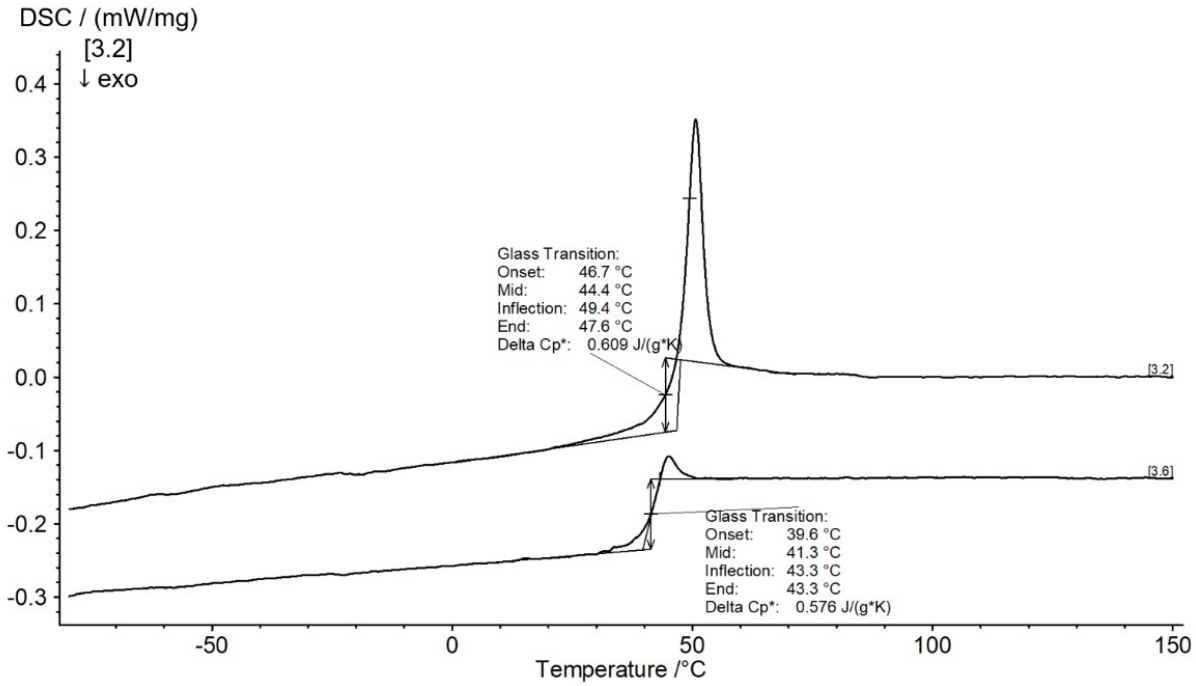

Figure S7. Differential scanning calorimetry (DSC) analysis of unmodified PLGA sample.

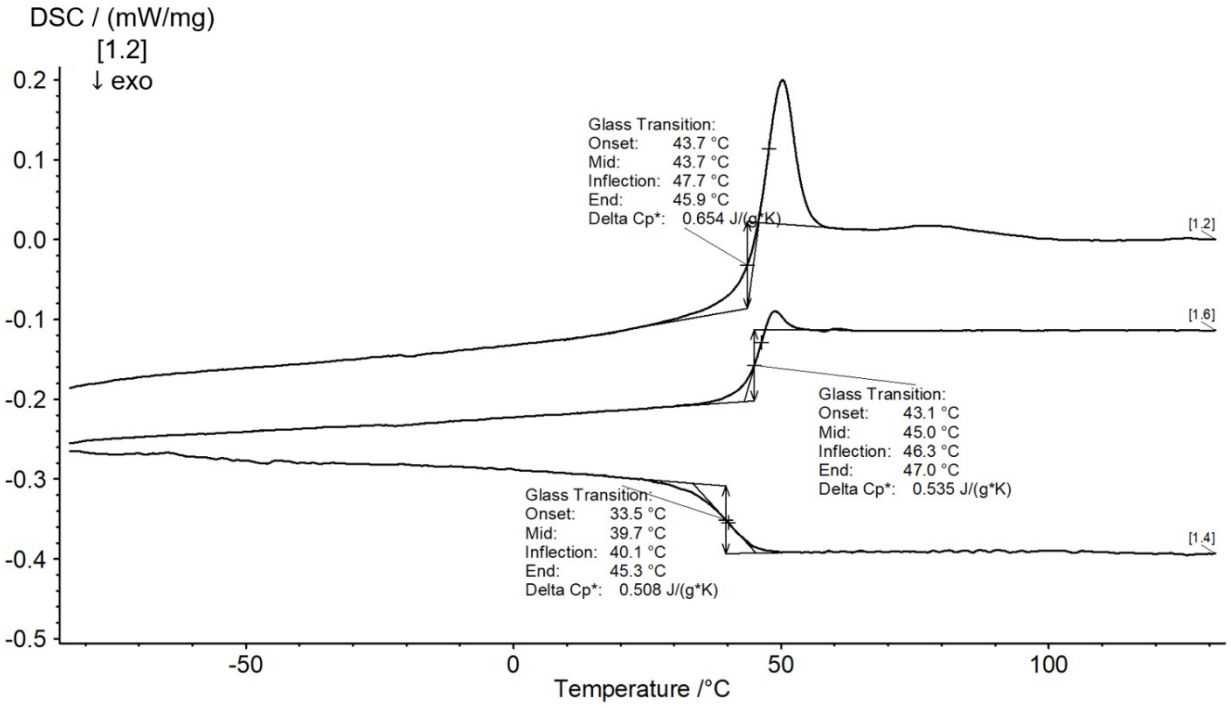

Figure S8. Differential scanning calorimetry (DSC) analysis of conjugate PLGA-5.

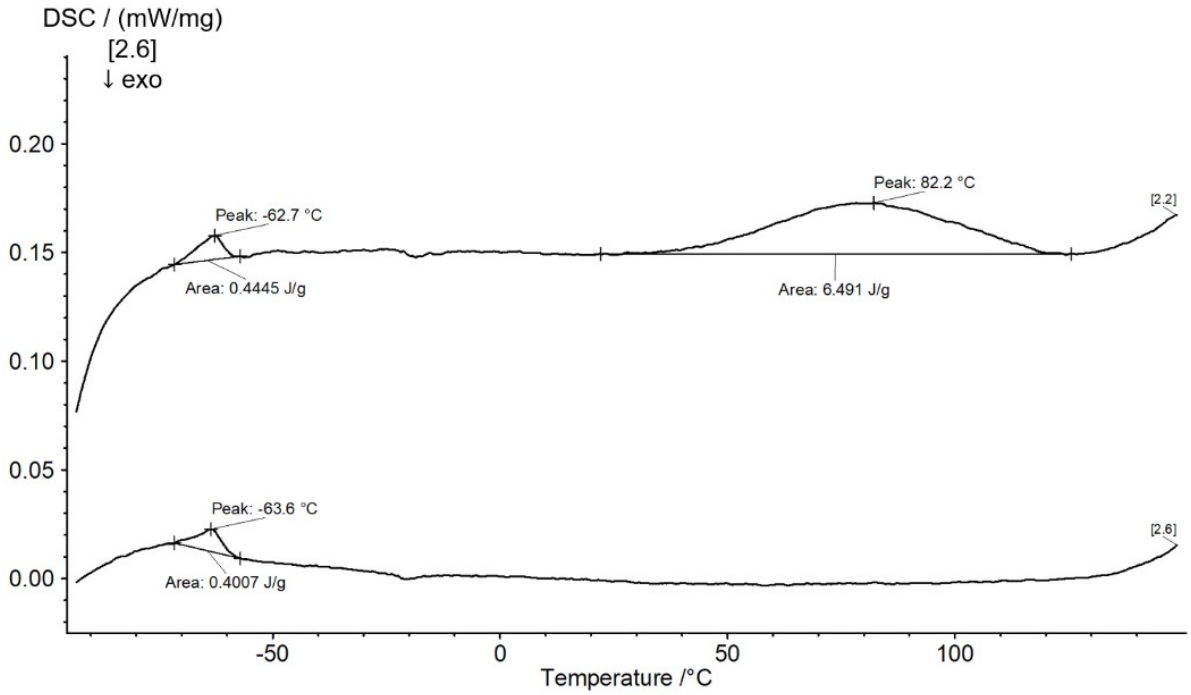

Figure S9. Differential scanning calorimetry (DSC) analysis of 1,8-naphthalimide 5.

1.1. Determination of the degree of substitution for PLGA-1,8-naphthalimide conjugates.

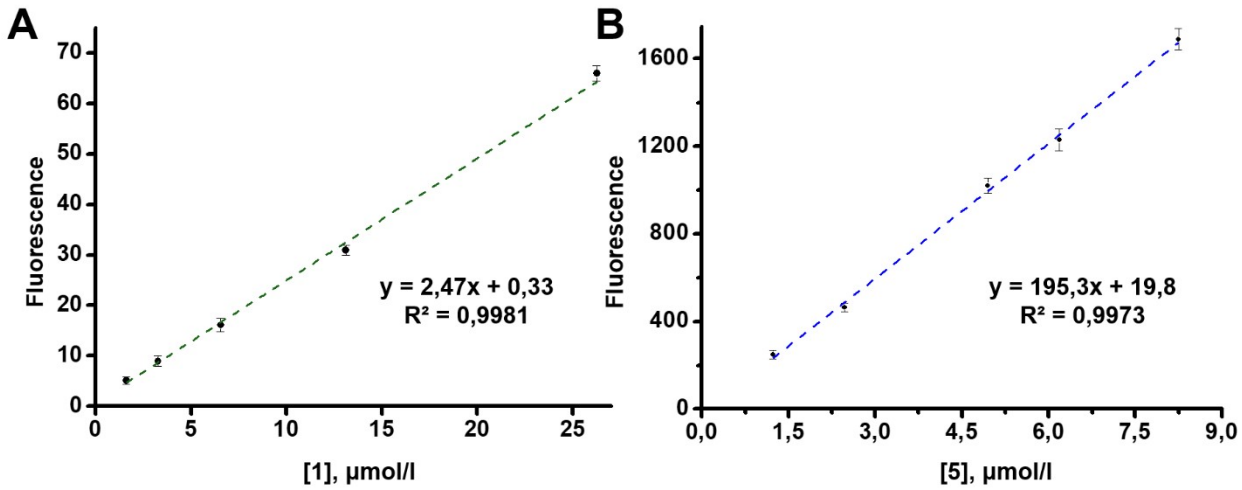

Figure S10. A) Calibration curve for dye **1** in water over the concentration range of 1.6 – 26.2 µmol/L in water. y = 2.47x + 0.33, R^2 = 0.9981. B) Calibration curve for dye **5** in water over the concentration range of 1.2 - 12.4 µmol/L in water. y = 195.3x + 19.8, R^2 = 0.9973.

Table S2. Degree of substitution in PLGA-1,8-naphthalimide conjugates determined by spectrofluorimetry

PLGA-1,8-naphthalimide conjugate	Degree of substitution, %
PLGA-1	41
PLGA-2	39
PLGA-3	42
PLGA-4	45
PLGA-5	43
PLGA-6	41
PLGA-7	39
PLGA-8	42

1.2. Confirmation of the purity of PLGA-1,8-naphthalimide conjugates

In order to verify the purity of the polymers obtained and to conduct further studies on their optical properties, it was necessary to determine the content of residual free fluorophore in the modified PLGA-naphthalimide 1-8 conjugate. For this purpose, high-performance liquid chromatography was utilised. The study was conducted for two fluorescent polymers, PLGA-**3** and PLGA-**5**, since free dyes and their conjugates dissolved excellently in acetonitrile. **Figure S11** and **Figure S12** illustrate two calibration curves for compounds **3** and **5**, which were utilised to ascertain the residual fluorophore content in the conjugate.

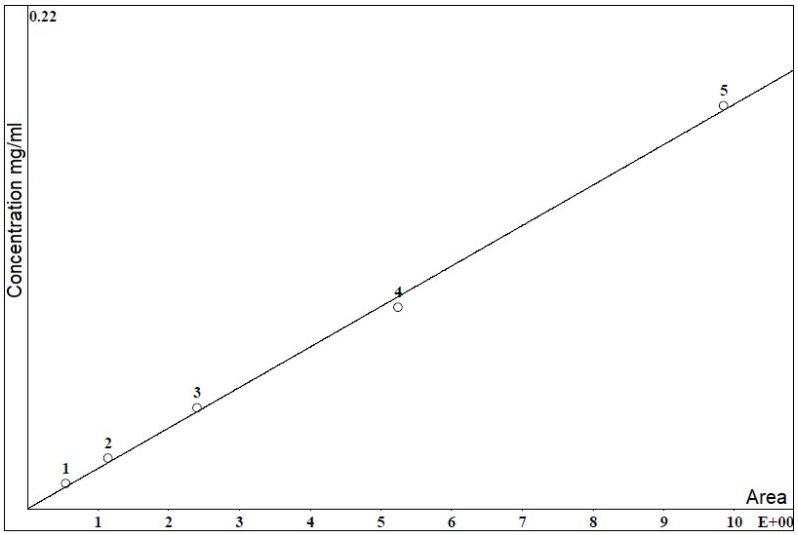

Figure S11. Calibration curve for dye **3** in the concentration range 0.0108–0.1720 mg/ml. Q = 0.03456×A, R = 0.9991. Dye elution time – 9.04 min.

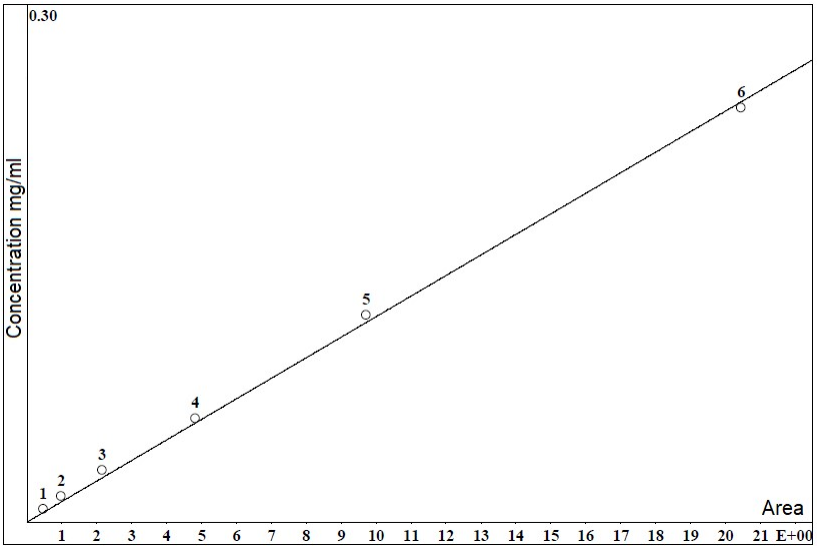

Figure S12. Calibration curve for dye **5** in the concentration range 0.0074–0.2360 mg/ml. Q = 0.0234×A, R = 0.9998. Dye elution time – 9.17 min.

The following figure illustrates a general view of the chromatogram of dye **3** and PLGA-**3** polymer (see **Figure S13**). During the processing of the chromatogram, a very low-intensity peak of free dye **3** was identified, the concentration of which, calculated from the calibration curve, was 0.0012 mg/ml. Consequently, the percentage content of free fluorophore **3** in the polymer corresponds to 0.012 wt.%.

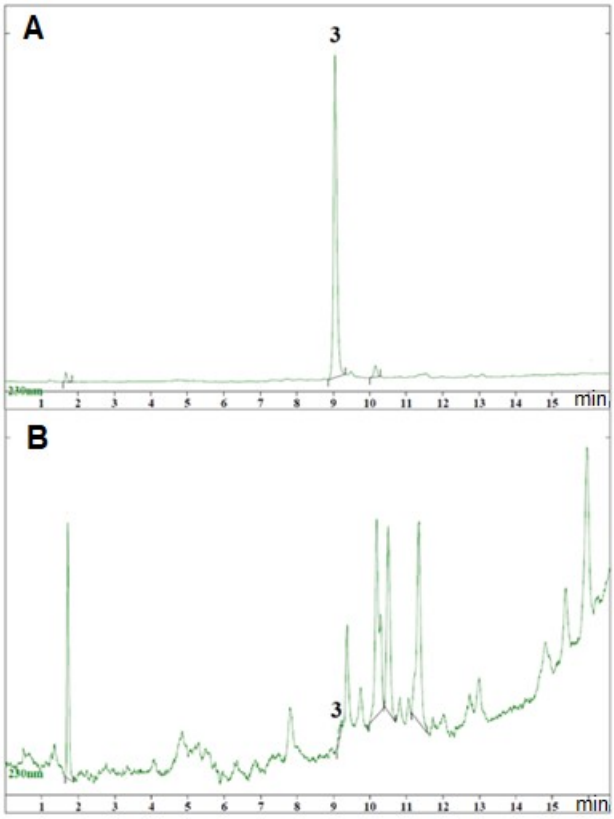

Figure S13. A) Chromatogram of dye 3 [3] = 0.086 mg/ml; B) Chromatogram of fluorescent polymer PLGA-3, [PLGA-3] = 10 mg/ml

A comparable study was conducted for dye **5** and PLGA-**5** polymer at a UV detector wavelength of 240 nm (see **Figure S14**). During the processing of the chromatogram, a peak of free dye 5 was identified, the concentration of which was calculated from the calibration curve to be 0.0013 mg/ml. Consequently, the fluorophore content in the polymer is 0.013 wt.%.

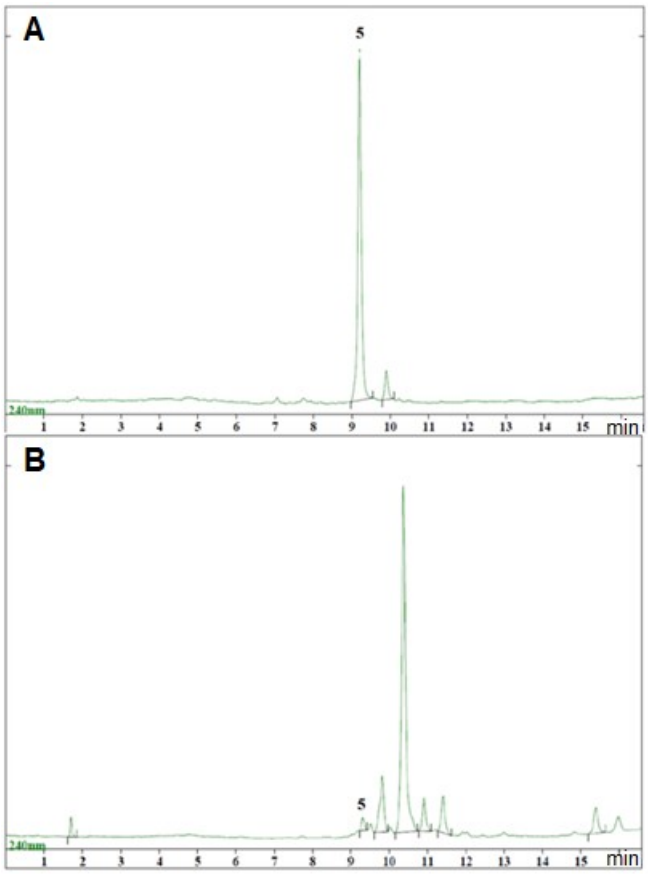

Figure S14. A) Chromatogram of dye 5, [5] = 0.0295 mg/ml; B) Chromatogram of fluorescent polymer PLGA-5, [PLGA-5] = 5.2 mg/ml

2. DFT calculations

The convergence tolerances for the geometry optimization procedure were energy change = 5.0×10^{-6} Eh, maximal gradient = 3.0×10^{-4} Eh/Bohr, RMS gradient = 1.0×10^{-4} Eh/Bohr, maximal displacement = 4.0×10^{-3} Bohr, and RMS displacement = 2.0×10^{-3} Bohr.

The parameters for ESD module were chosen to be: spectral lineshape – Lorentzian, spectral range – 12500 to 25000 cm^{-1} (400 to 800 nm), linewidth – 2500 cm^{-1}, spectral resolution – 100.

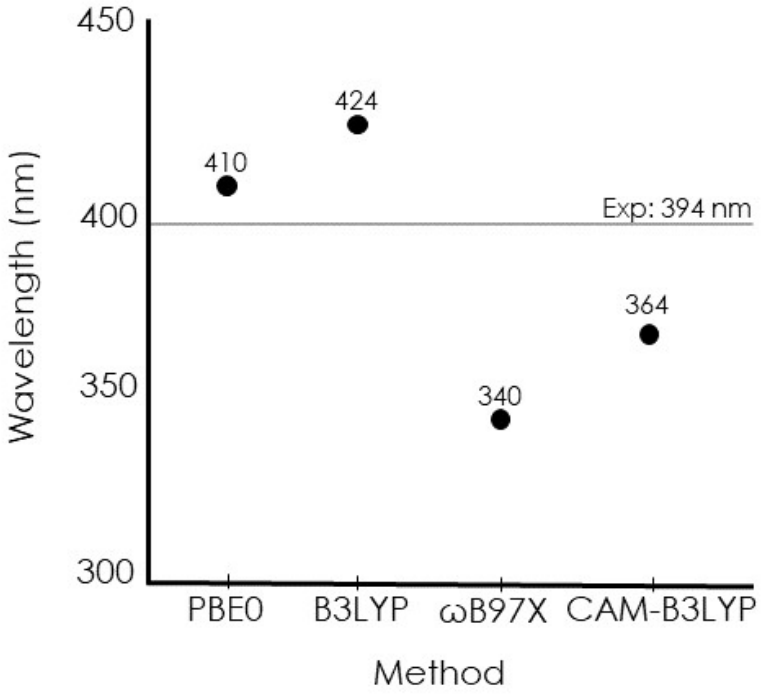

Figure S15. Calculated absorption maxima for compound **1** plotted against the experimental wavelength (gray horizontal line)

2.1. The experimental and TD-DFT/ESD calculated absorption and fluorescence spectra

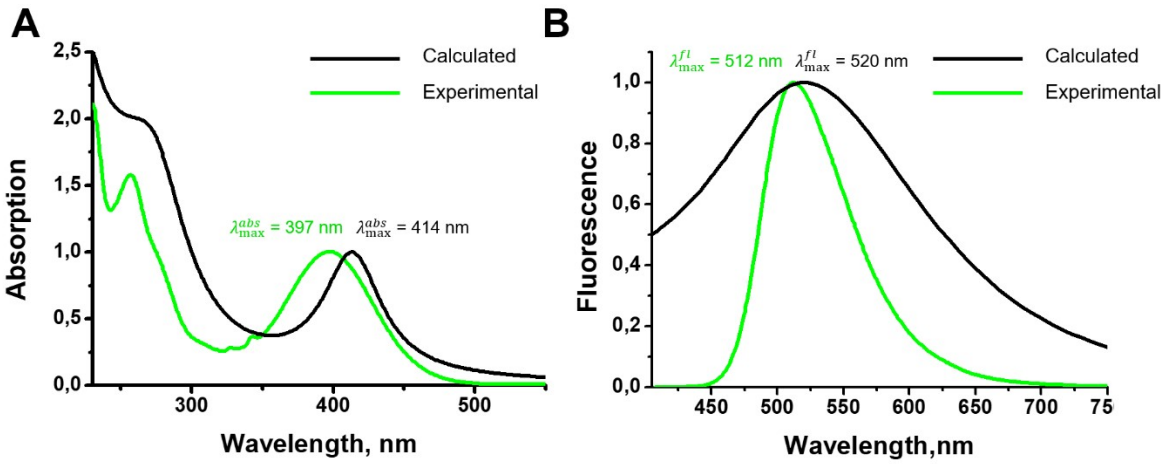

Figure S16. A) The experimental and TD-DFT calculated UV-Vis absorption spectra of the compound **2**. B) The experimental and ESD calculated luminescence spectra of the compound **2**

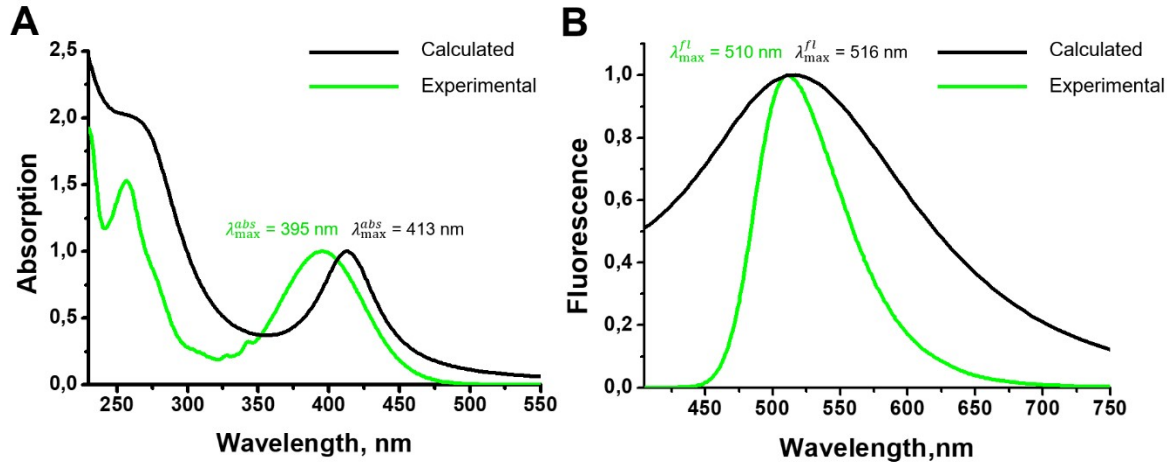

Figure S17. A) The experimental and TD-DFT calculated UV-Vis absorption spectra of the compound **3**. B) The experimental and ESD calculated luminescence spectra of the compound **3**

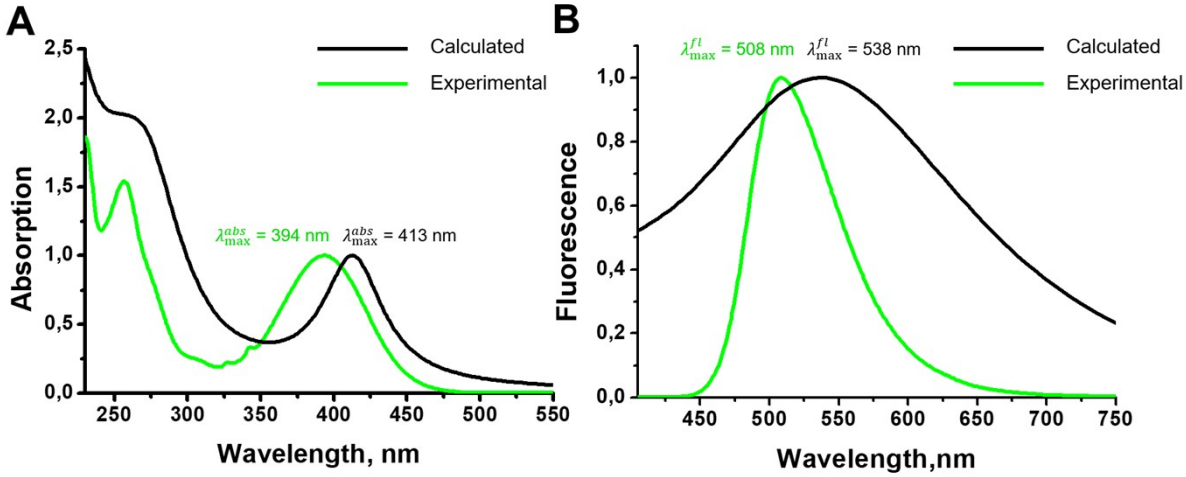

Figure S18. A) The experimental and TD-DFT calculated UV-Vis absorption spectra of the compound **4**. B) The experimental and ESD calculated luminescence spectra of the compound **4**

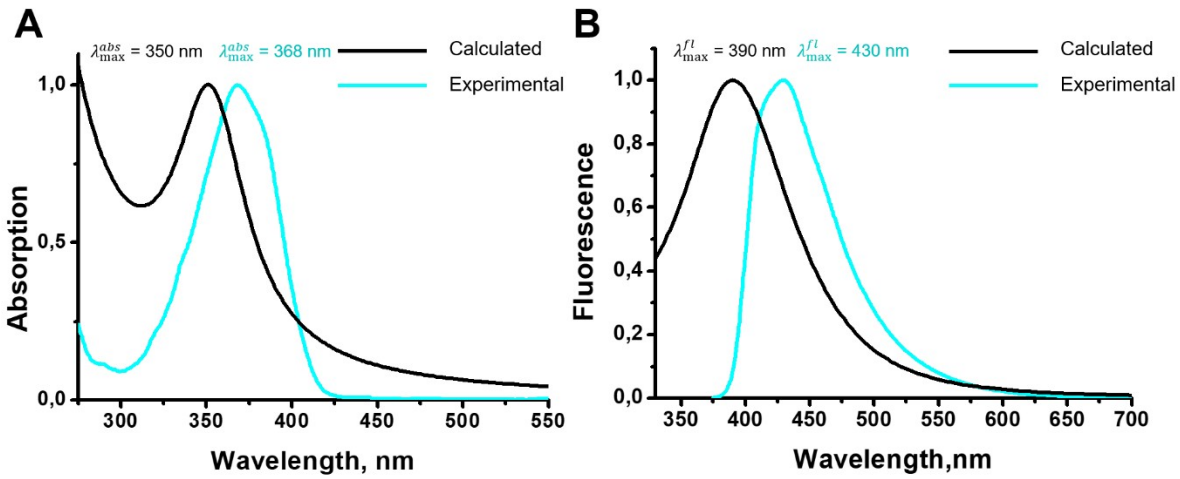

Figure S19. A) The experimental and TD-DFT calculated UV-Vis absorption spectra of the compound **6**. B) The experimental and ESD calculated luminescence spectra of the compound **6**

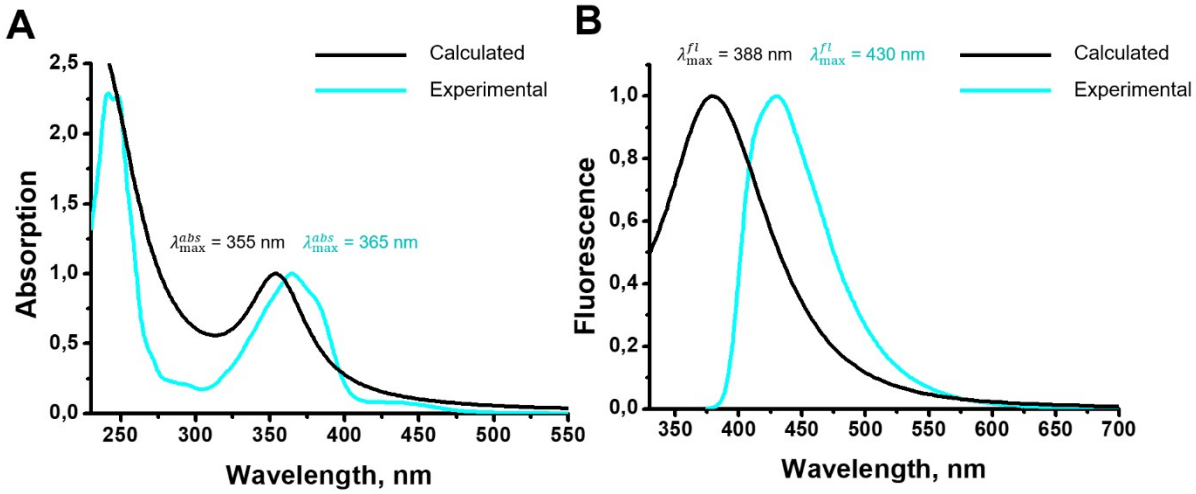

Figure S20. A) The experimental and TD-DFT calculated UV-Vis absorption spectra of the compound **7**. B) The experimental and ESD calculated luminescence spectra of the compound **7**

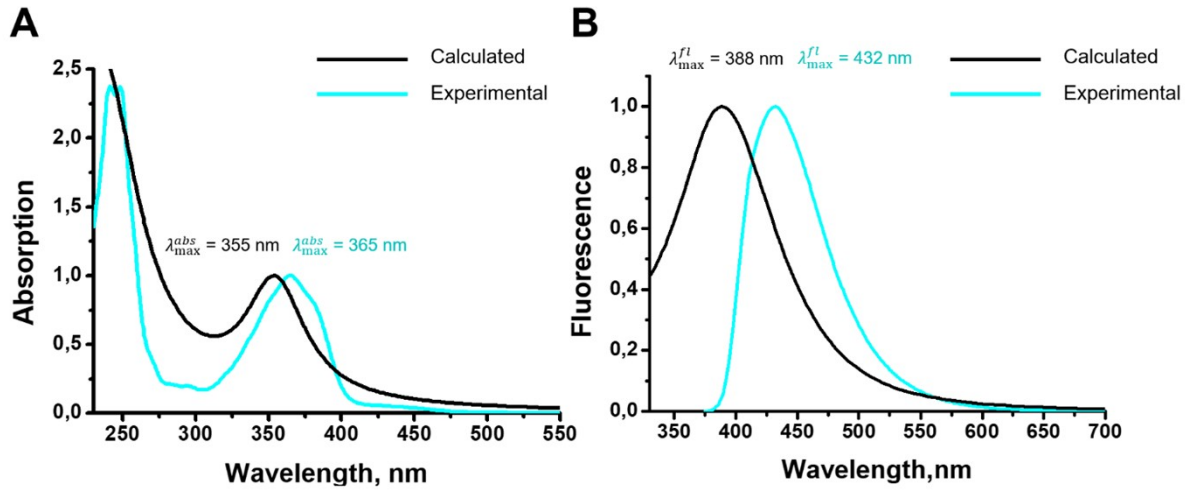

Figure S21. A) The experimental and TD-DFT calculated UV-Vis absorption spectra of the compound **8**. B) The experimental and ESD calculated luminescence spectra of the compound **8**

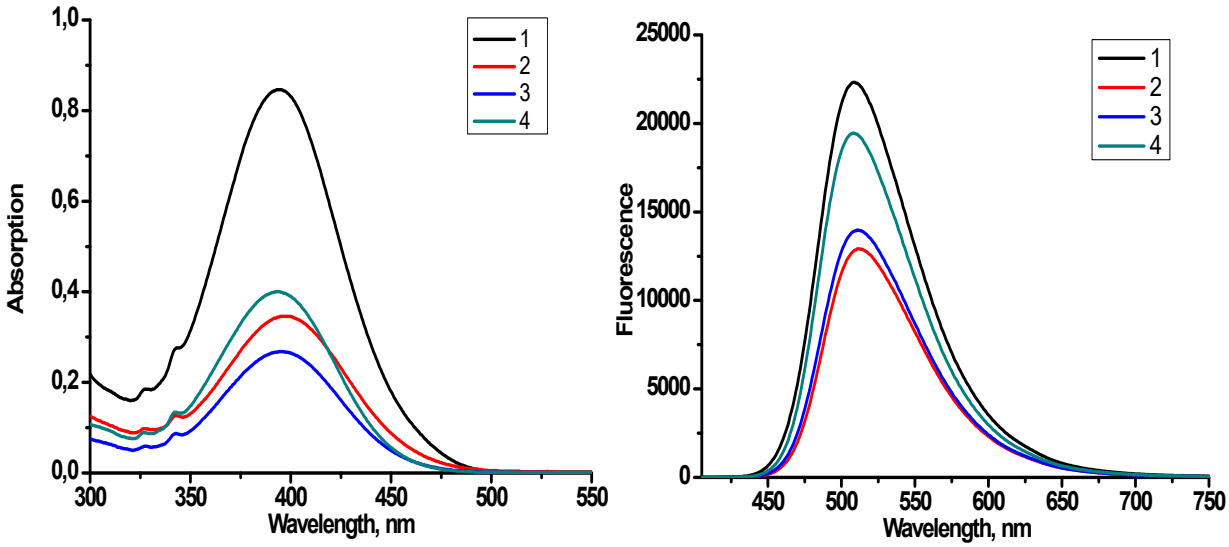

Figure S22. Absorption and fluorescence spectra of fluorophores **1-4** in CH_2Cl_2. Concentration of fluorophores **1-4** – 1,2 · 10^{-2} mg/ml

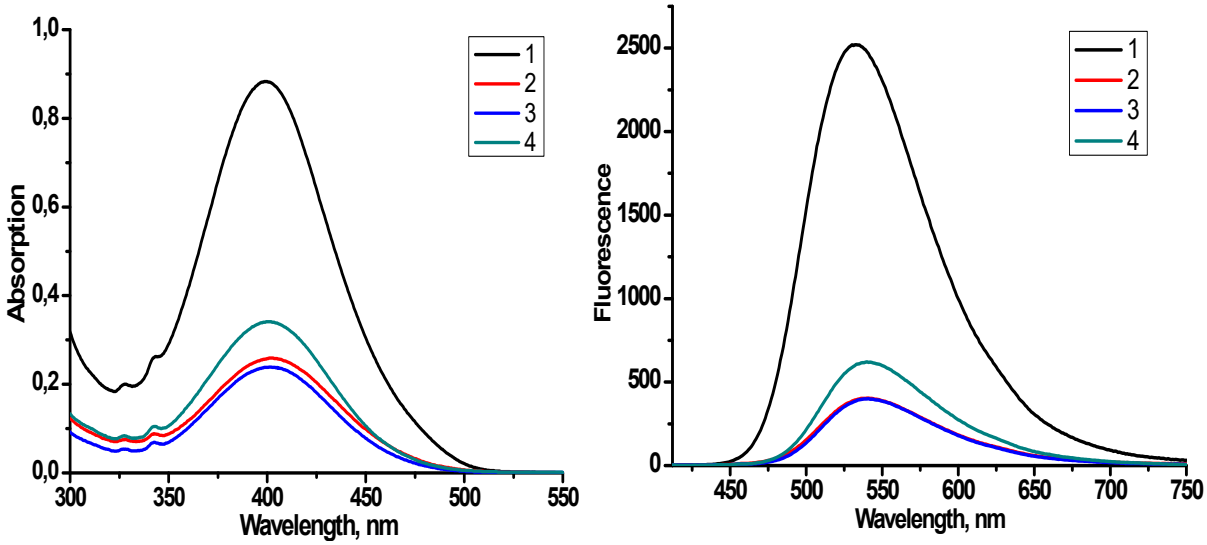

Figure S23. Absorption and fluorescence spectra of fluorophores **1-4** in DMSO. Concentration of fluorophores **1-4** – 1,2 · 10^{-2} mg/ml

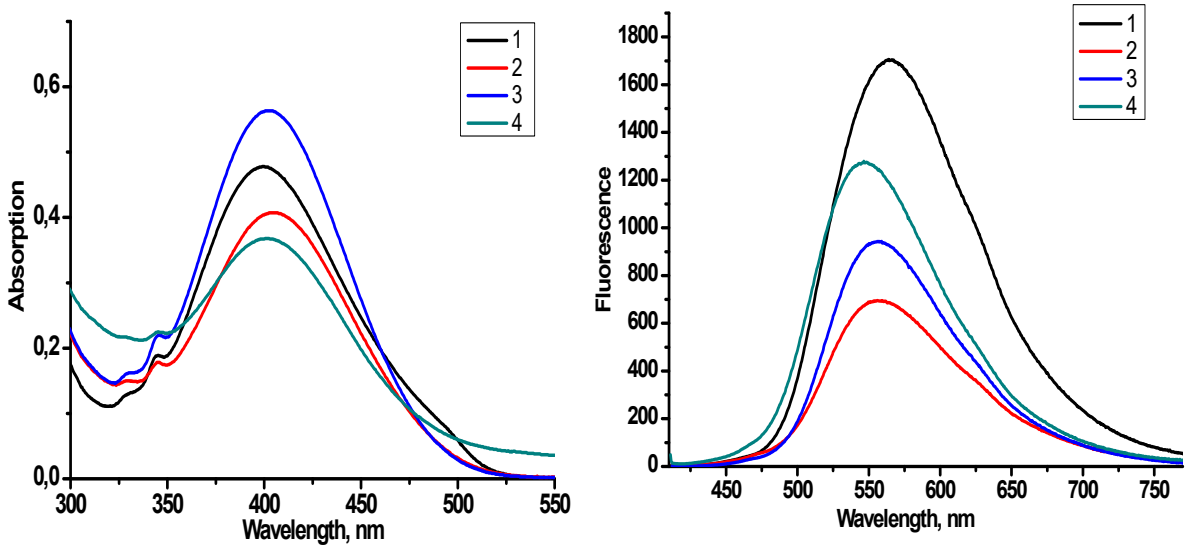

Figure S24. Absorption and fluorescence spectra of fluorophores **1-4** in H_2O. Concentration of fluorophores **1-4** – 1,2 · 10^{-2} mg/ml

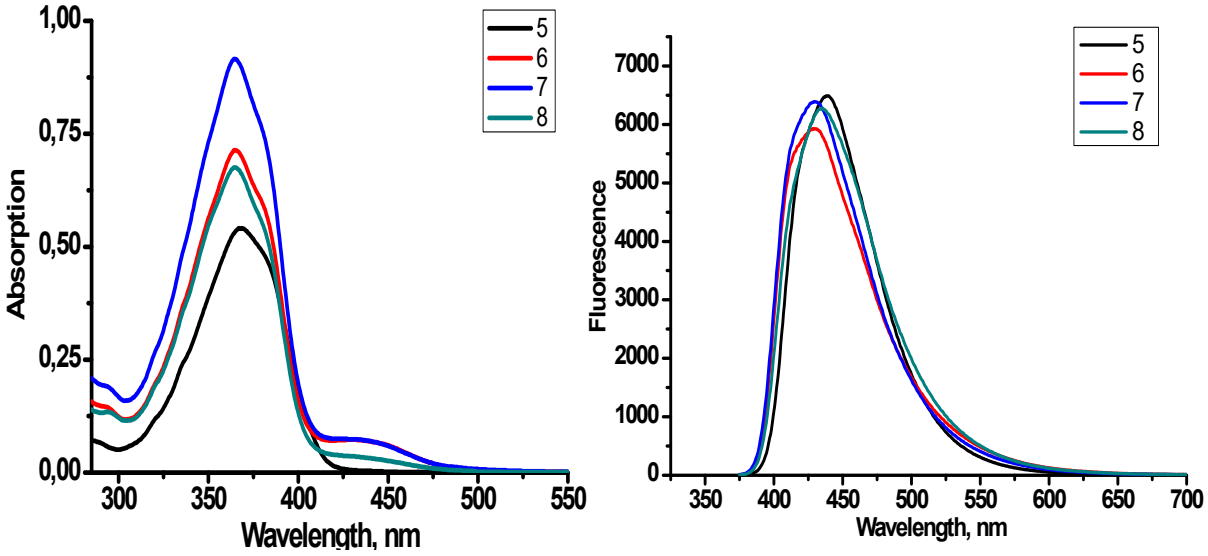

Figure S25. Absorption and fluorescence spectra of fluorophores **5-8** in CH_2Cl_2. Concentration of fluorophores **5-8** – 1,2 · 10^{-2} mg/ml

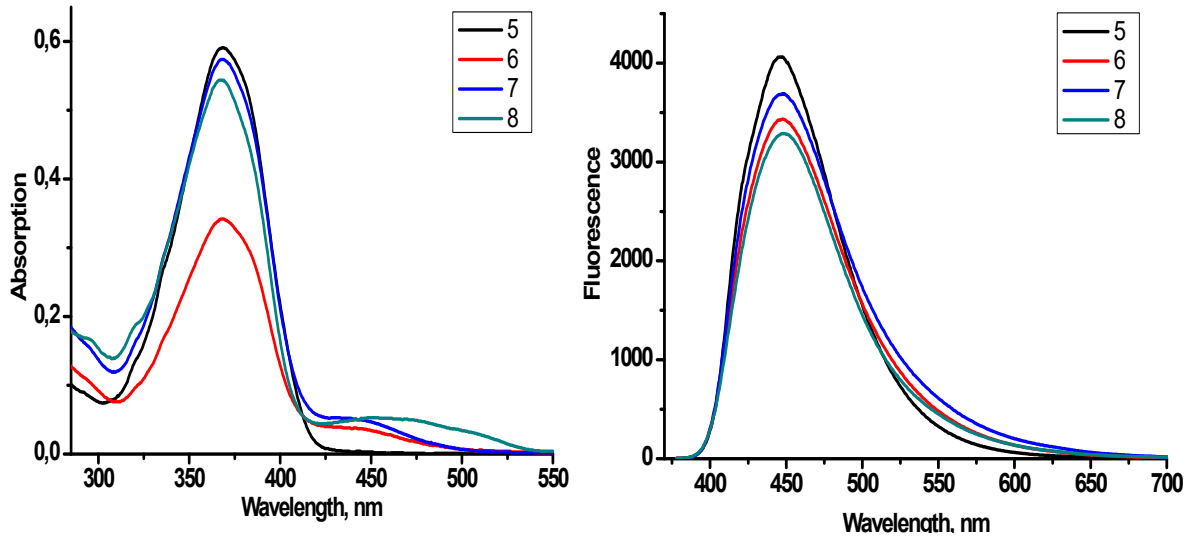

Figure S26. Absorption and fluorescence spectra of fluorophores **5-8** in DMSO. Concentration of fluorophores **5-8** – $1{,}2 \cdot 10^{-2}$ mg/ml

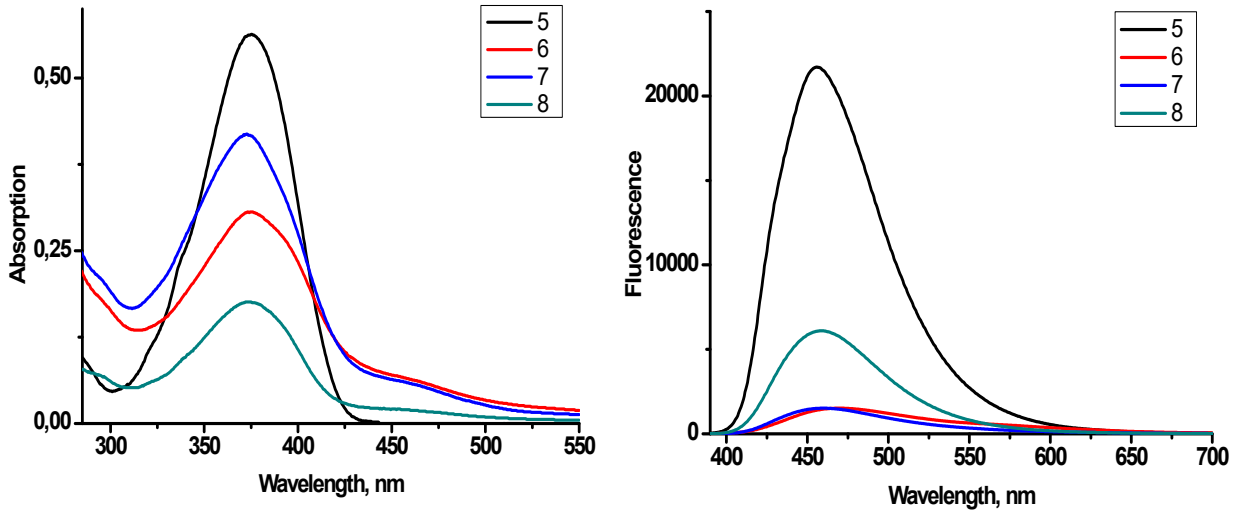

Figure S27. Absorption and fluorescence spectra of fluorophores **5-8** in H_2O. Concentration of fluorophores **5-8** – $1{,}2 \cdot 10^{-2}$ mg/ml

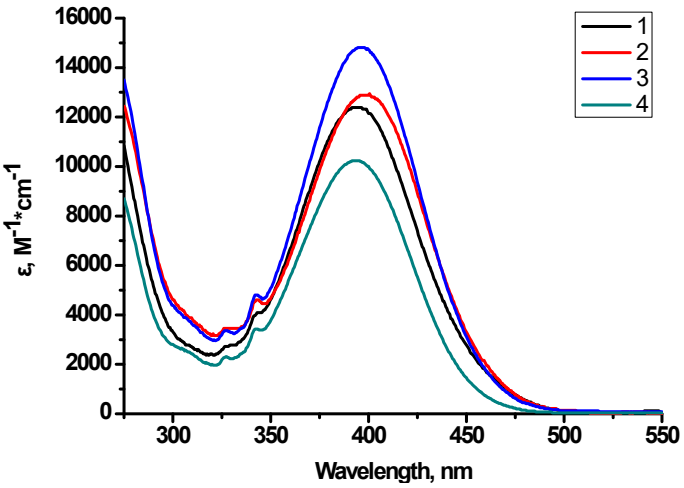

Figure S28. Wavelength dependence of extinction coefficient for fluorophores **1–4** in CH_2Cl_2

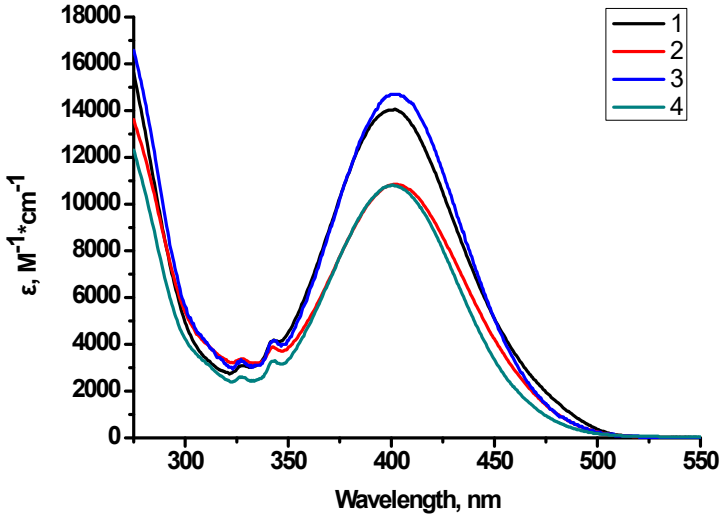

Figure S29. Wavelength dependence of extinction coefficient for fluorophores **1–4** in DMSO

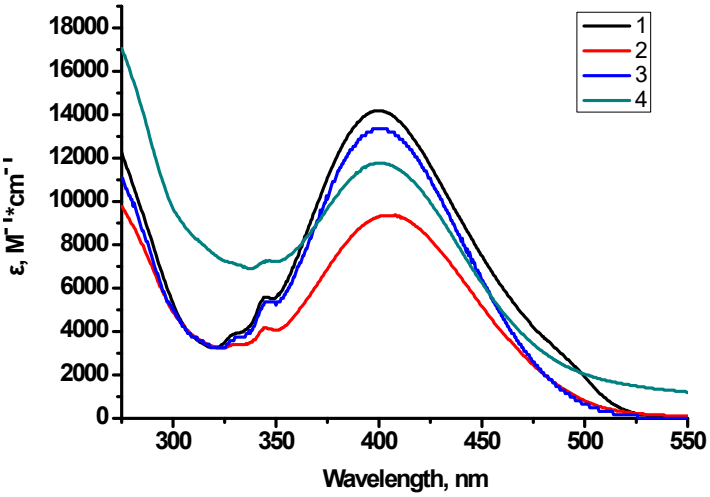

Figure S30. Wavelength dependence of extinction coefficient for fluorophores **1–4** in H_2O

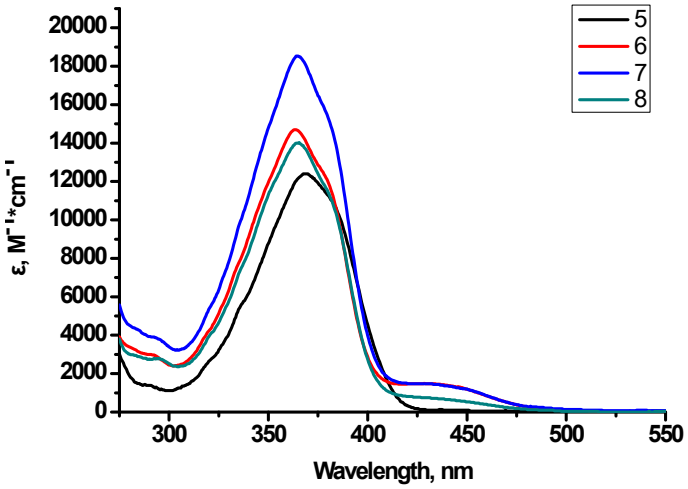

Figure S31. Wavelength dependence of extinction coefficient for fluorophores **5-8** in CH_2Cl_2

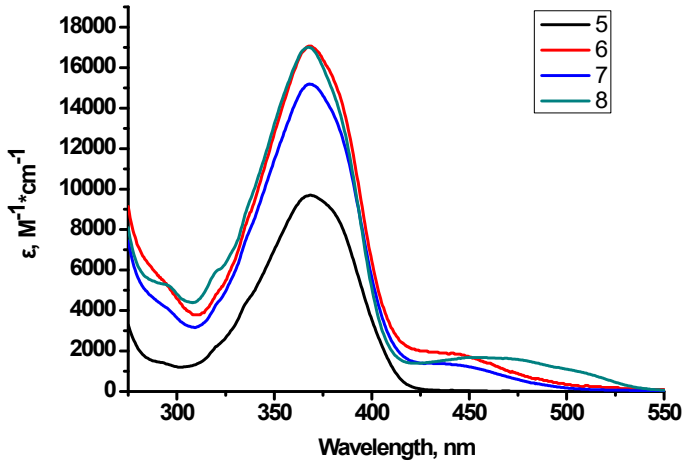

Figure S32. Wavelength dependence of extinction coefficient for fluorophores **5-8** in DMSO

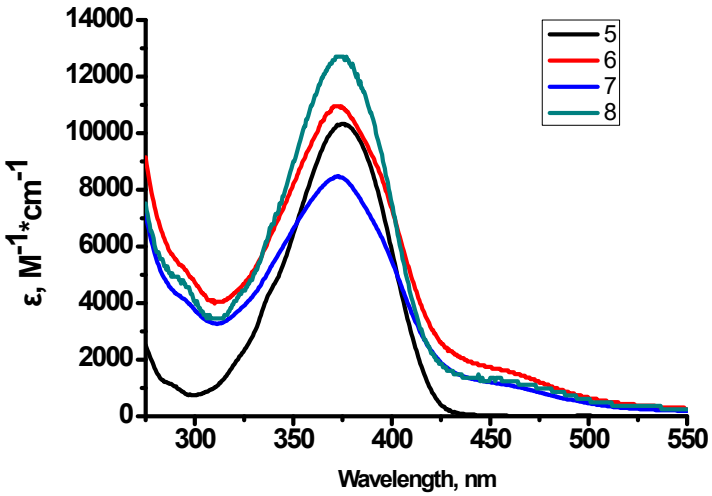

Figure S33. Wavelength dependence of extinction coefficient for fluorophores **5-8** in H_2O

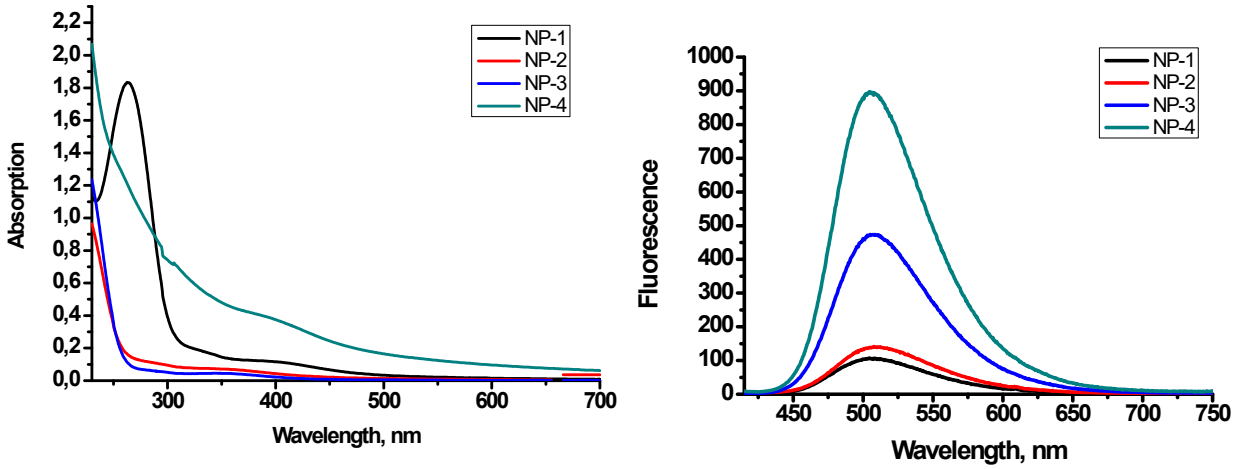

Figure S34. Absorption and fluorescence spectra for nanoparticles PLGA-fluorophore **1-4**. Concentration of NPs – 2,5 mg/ml

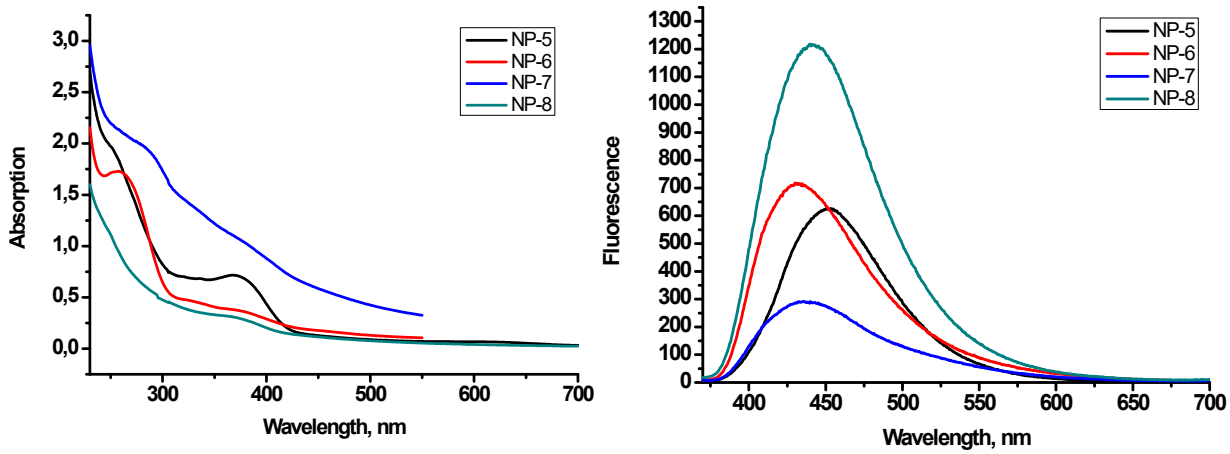

Figure S35. Absorption and fluorescence spectra for nanoparticles PLGA-fluorophore **5-8**. Concentration of NPs – 2,5 mg/ml

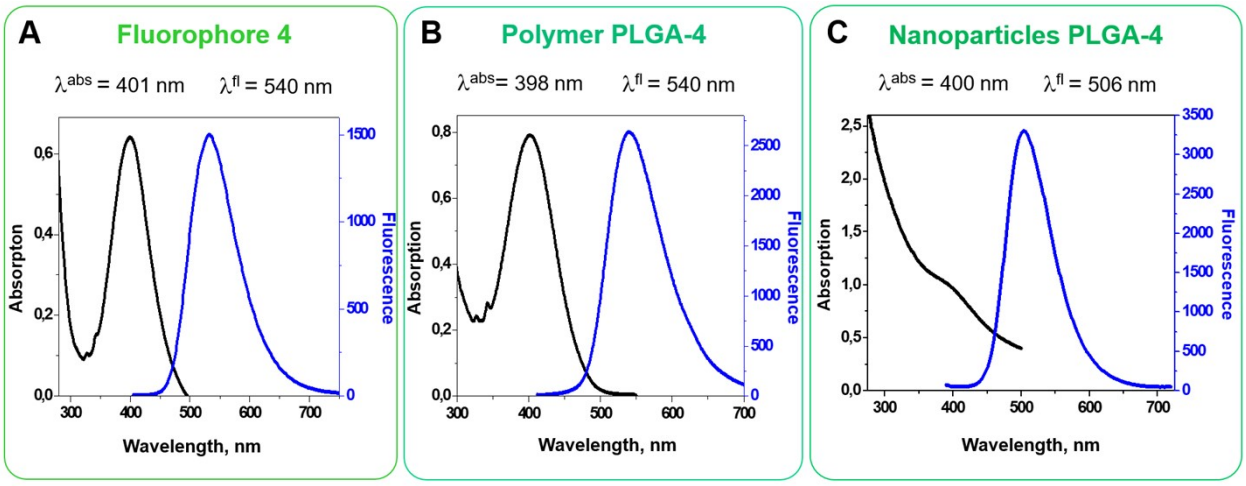

Figure S36. A – Absorption and fluorescence spectra of fluorophore 4 in DMSO, concentration [4] – 19.6 mg/ml. B – Absorption and fluorescence spectra of PLGA-4 polymer in DMSO, concentration [PLGA-4] – 12.0 mg/ml. C – Absorption and fluorescence spectra of PLGA-4 nanoparticles in water, concentration [PLGA-4] – 2.5 mg/ml.

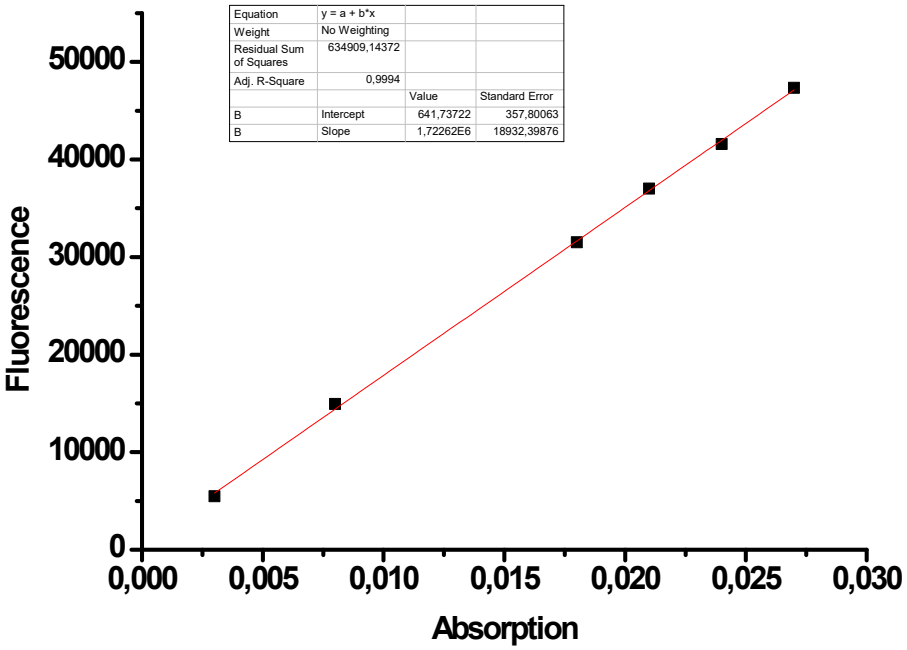

Figure S37. Fluorescence intensity dependence of absorbance for Coumarin 6. y = 1 731 025,7407x + 371,8702, R^2 = 0,9994

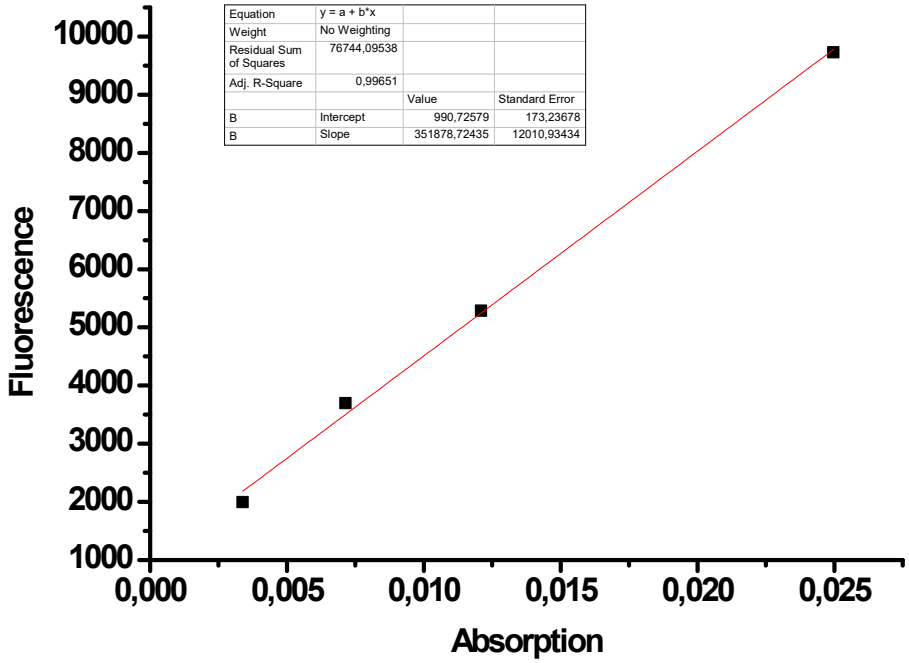

Figure S38. Fluorescence intensity dependence of absorbance for nanoparticles PLGA-**1**. y = 351 878,7244x + 990,7258, R^2 = 0, 9997

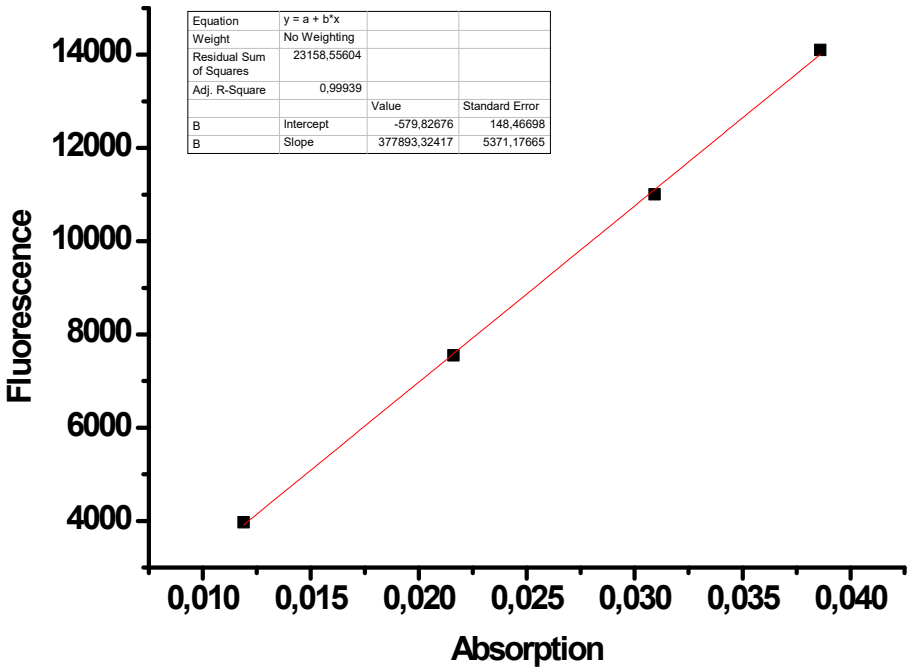

Figure S39. Fluorescence intensity dependence of absorbance for nanoparticles PLGA-**2**. y = 377893x - 579,83, R^2 = 0,9994

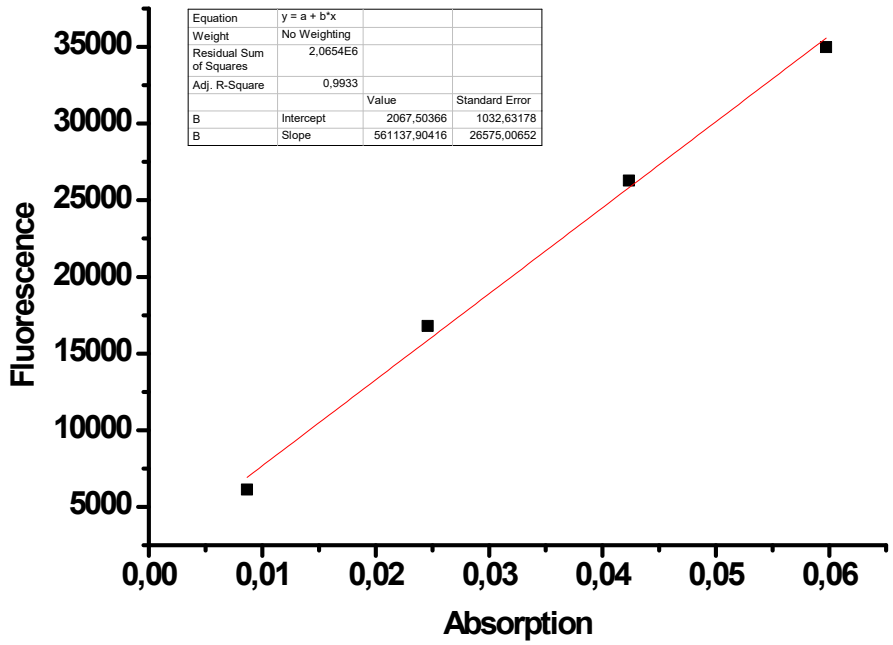

Figure S40. Fluorescence intensity dependence of absorbance for nanoparticles PLGA-**3**. y = 561138x + 2067,5, R^2 = 0,9933

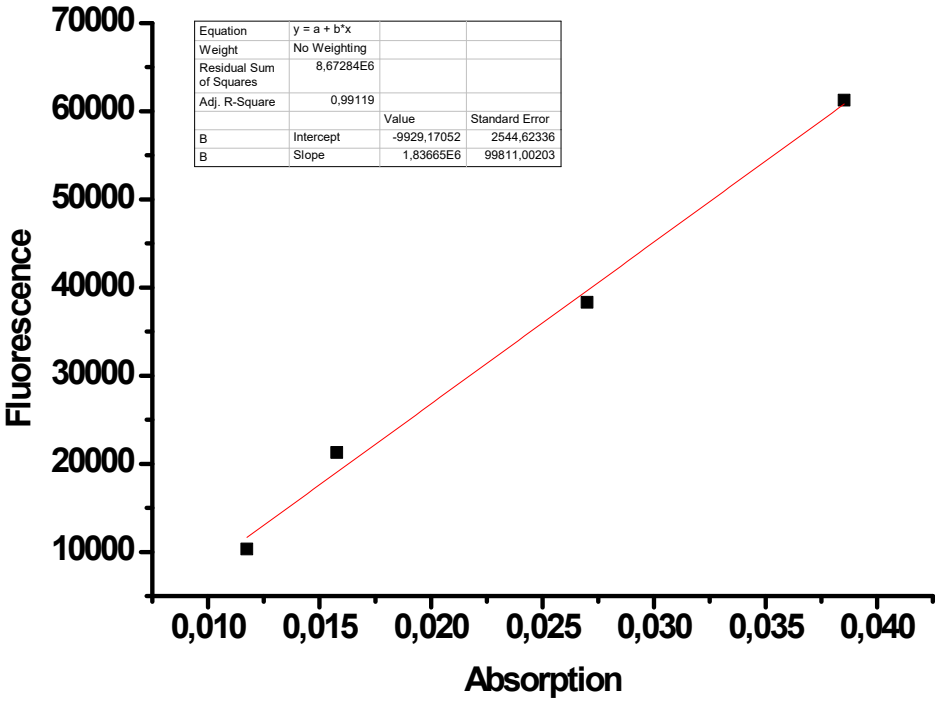

Figure S41. Fluorescence intensity dependence of absorbance for nanoparticles PLGA-**4**.

y = 1 836 650,1484x - 9 929,1696, R^2 = 0,9912

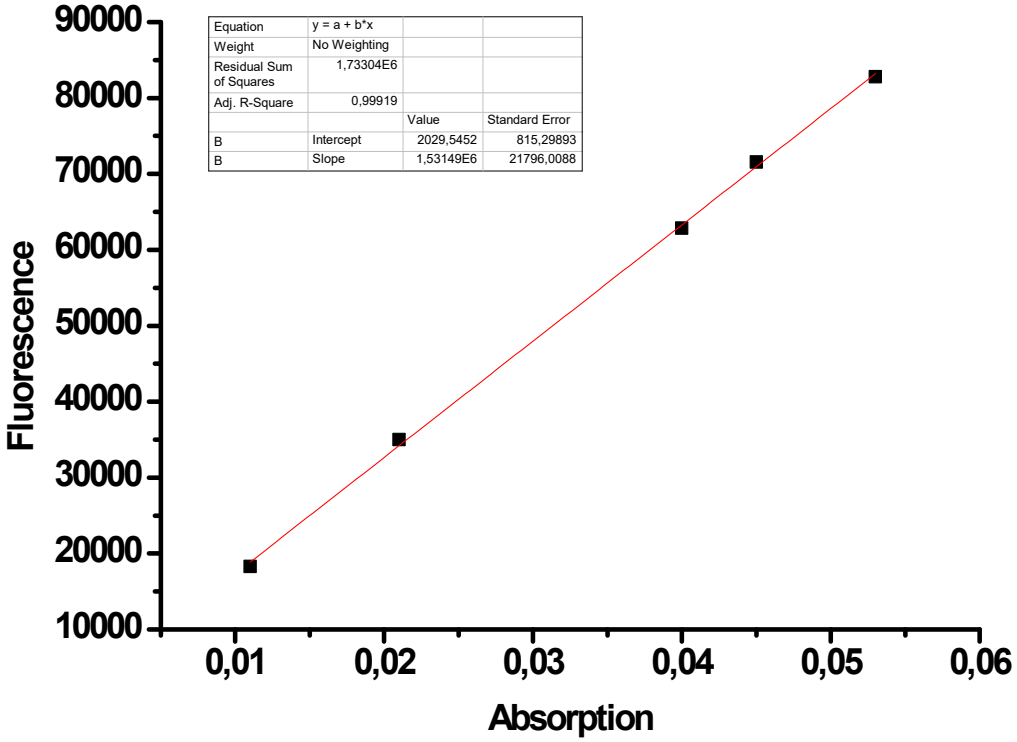

Figure S42. Fluorescence intensity dependence of absorbance for quinine sulfate.

y = 1 547 545,9646x + 1 720,4130, R^2 = 0,9992

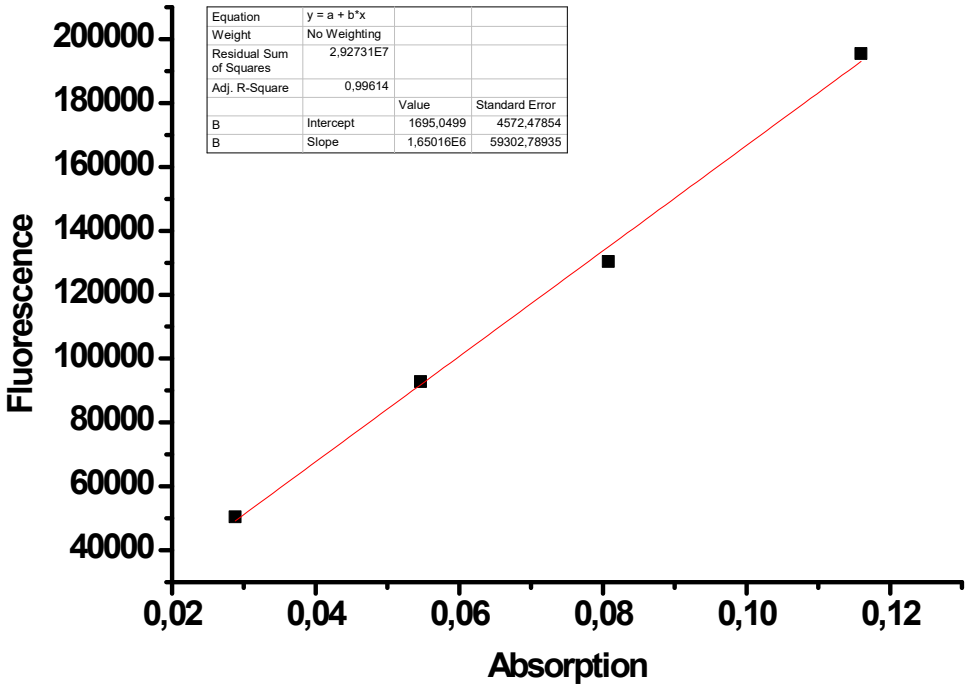

Figure S43. Fluorescence intensity dependence of absorbance for nanoparticles PLGA-**5**. y = 1 650 162,7829x + 1 695,0499, R^2 = 0,9961

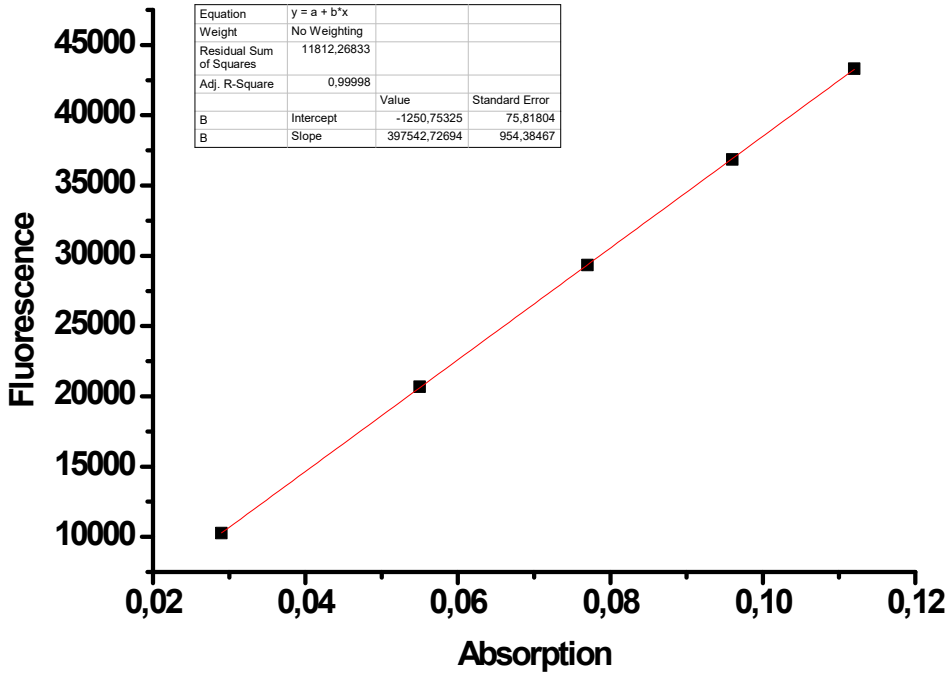

Figure S44. Fluorescence intensity dependence of absorbance for nanoparticles PLGA-**6**. y = 397 542,7269x - 1 250,7532, R^2 = 1,0000

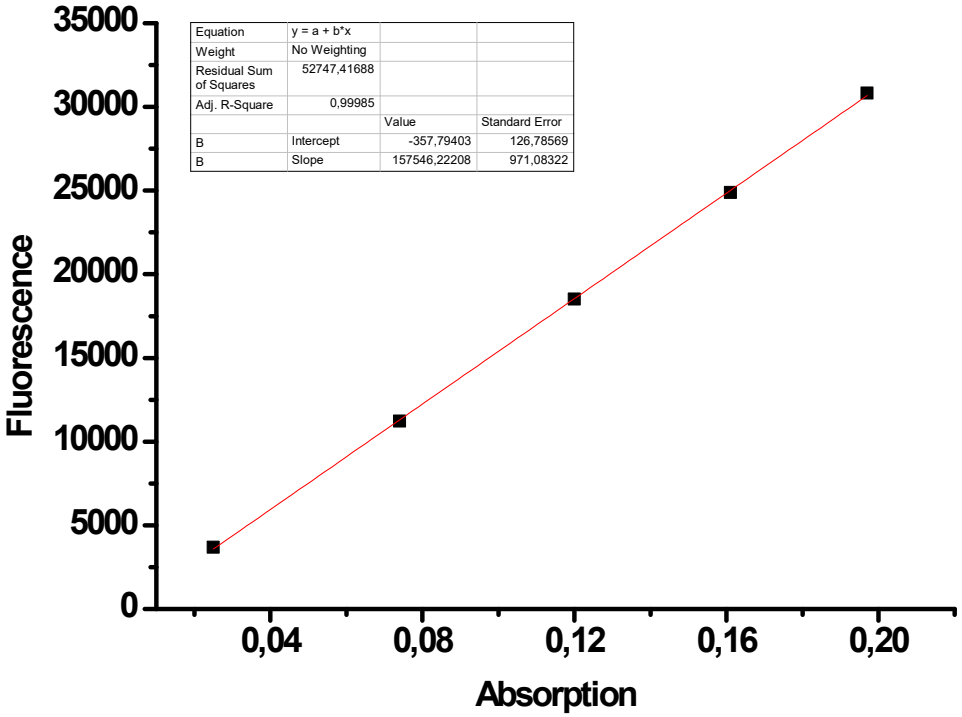

Figure S45. Fluorescence intensity dependence of absorbance for nanoparticles PLGA-**7**. y = 157546x - 357,79, R^2 = 0,9999

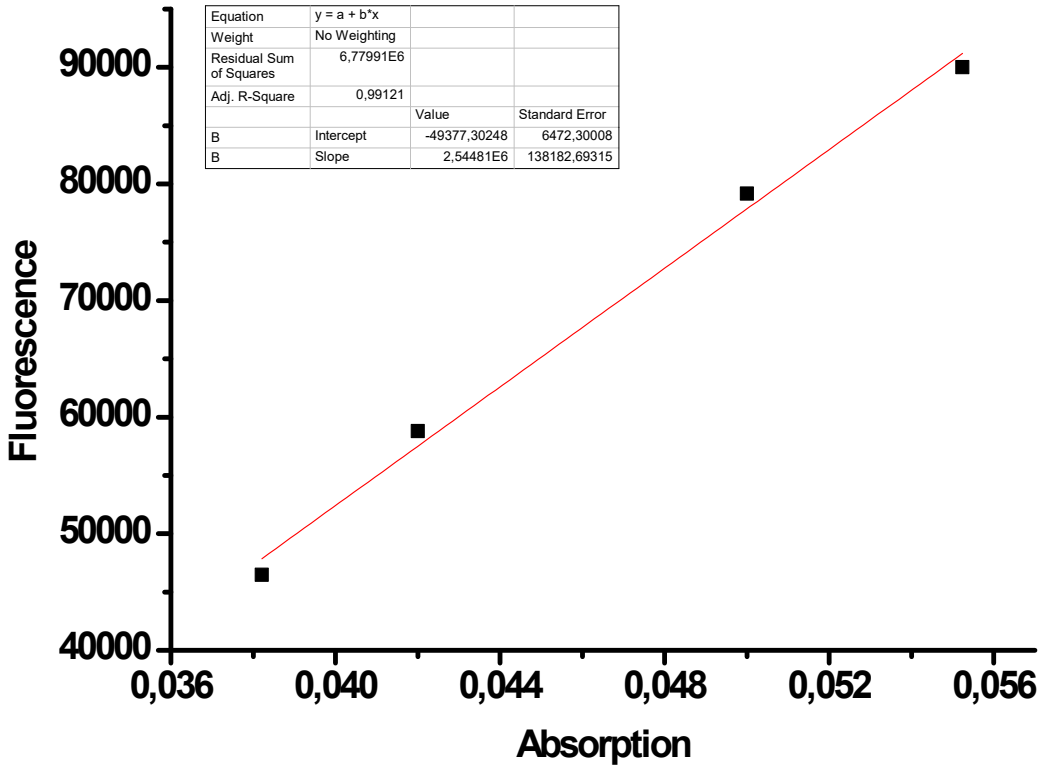

Figure S46. Fluorescence intensity dependence of absorbance for nanoparticles PLGA-**8**. y = 2 544 815,4164x - 49 377,3799, R^2 = 0,9912

Table S3. Spectral properties of the obtained dyes and brightness of nanoparticles in comparison with the properties of common fluorescent markers

	Dye	λ_{abs}, nm	λ_{fl}, nm	Stokes shift, nm	Molar extinction coefficient of dye, ε, $l \cdot mol^{-1} \cdot cm^{-1}$	Fluorescence quantum yield of dye, %	Brightness of NP, per mg of NP material
1	Sulfo-Cy3	548	563	15	162000	10	$2{,}003 \cdot 10^{19}$
2	Cy3	544	557	13	133000	7	$2{,}547 \cdot 10^{19}$
3	Cy5	646	658	12	200000	40	$2{,}128 \cdot 10^{19}$
4	Fluorescein isothiocyanate	500	541	41	92300	97	$6{,}690 \cdot 10^{17}$
5	**4**	400	546	146	11740	3,2	$7{,}469 \cdot 10^{20}$
6	**5**	375	457	82	12200	72	$1{,}066 \cdot 10^{21}$
7	**8**	374	457	83	12500	78	$8{,}080 \cdot 10^{20}$

Table S4. Average lifetimes of excited states of fluorophores in free form and in nanoparticles

Fluorophore	Excited state lifetime of free dye, ns	Excited state lifetime of dye in the nanoparticles, ns
1	0,45	5,58
2	0,36	4,00
3	0,40	4,07
4	0,68	5,35
5	4,68	4,56
6	5,05	4,93
7	5,50	4,57
8	5,59	5,59

Table S5. Dependence of the average size of nanoparticles (nm) from PLGA-**4** and PLGA-**8** polymers on time in experiments to study stability during incubation at 37 °C in PBS, RPMI-1640 and DMEM media.

Nanoparticle type	Time, h	Nanoparticle size and size distribution	
		Average diameter, nm	PDI
		PBS	
PLGA-4	0	125,9 ± 1,3	0,139 ± 0,030
	1	138,0 ± 1,7	0,156 ± 0,023
	2	139,2 ± 2,3	0,203 ± 0,008
	3	131,0 ± 2,0	0,180 ± 0,016
	4	132,2 ± 2,1	0,194 ± 0,012
	5	142,4 ± 2,0	0,172 ± 0,008
	6	132,7 ± 2,0	0,161 ± 0,023
	24	106,7 ± 2,3	0,173 ± 0,018
	48	130,1 ± 1,9	0,183 ± 0,015
PLGA-8	0	126,8 ± 3,0	0,113 ± 0,022
	1	130,9 ± 3,5	0,119 ± 0,005
	2	110,6 ± 1,5	0,105 ± 0,002
	3	111,8 ± 2,0	0,1127 ± 0,030
	4	109,9 ± 1,0	0,106 ± 0,045
	5	109,4 ± 2,2	0,124 ± 0,008
	6	112,6 ± 2,1	0,112 ± 0,032
	24	125,4 ± 2,2	0,151 ± 0,013
	48	110,4 ± 2,0	0,133 ± 0,021
		RPMI-1640	
PLGA-4	0	128,2 ± 2,3	0,140 ± 0,011
	1	128,1 ± 2,4	0,157 ± 0,006
	2	133,4 ± 2,0	0,179 ± 0,019
	3	133,7 ± 2,2	0,127 ± 0,026
	4	133,8 ± 3,0	0,139 ± 0,008
	5	132,1 ± 2,5	0,150 ± 0,012
	6	131,8 ± 2,0	0,153 ± 0,031
	24	129,7 ± 2,0	0,183 ± 0,025
	48	188,7 ± 1,1	0,365 ± 0,016
PLGA-8	0	113,7 ± 1,9	0,111 ± 0,004

	1	109,6 ± 2,0	0,112 ± 0,009
	2	116,7 ± 2,4	0,122 ± 0,033
	3	113,8 ± 2,1	0,200 ± 0,010
	4	117,3 ± 2,3	0,154 ± 0,026
	5	111,6 ± 2,4	0,123 ± 0,009
	6	112,6 ± 2,0	0,130 ± 0,011
	24	113,6 ± 2,2	0,171 ± 0,028
	48	247,1 ± 3,8	0,379 ± 0,012
		DMEM	
	0	129,1 ± 2,0	0,139 ± 0,008
	1	128,7 ± 2,5	0,136 ± 0,028
	2	128,7 ± 3,0	0,172 ± 0,006
	3	129,3 ± 2,2	0,196 ± 0,011
PLGA-4	4	130,8 ± 2,5	0,203 ± 0,0004
	5	131,1 ± 2,3	0,187 ± 0,013
	6	130,9 ± 3,0	0,196 ± 0,014
	24	138,6 ± 2,7	0,192 ± 0,018
	48	129,1 ± 3,6	0,204 ± 0,003
	0	115,9 ± 2,0	0,102 ± 0,015
	1	116,4 ± 2,2	0,105 ± 0,014
	2	114,5 ± 3,1	0,108 ± 0,016
	3	112,2 ± 2,4	0,116 ± 0,007
PLGA-8	4	116,1 ± 2,1	0,115 ± 0,009
	5	113,4 ± 2,3	0,148 ± 0,012
	6	110,3 ± 2,2	0,138 ± 0,016
	24	113,8 ± 2,5	0,135 ± 0,024
	48	115,9 ± 2,1	0,144 ± 0,030

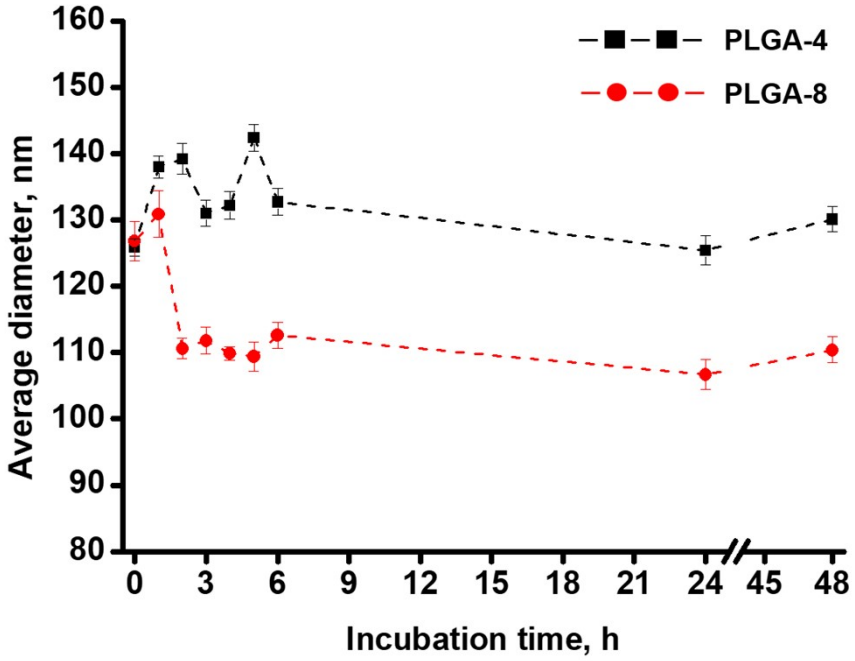

Figure S47. Dependence of the average size of nanoparticles (nm) from PLGA-**4** and PLGA-**8** polymers on time in experiments to study stability during incubation at 37 °C in PBS media.

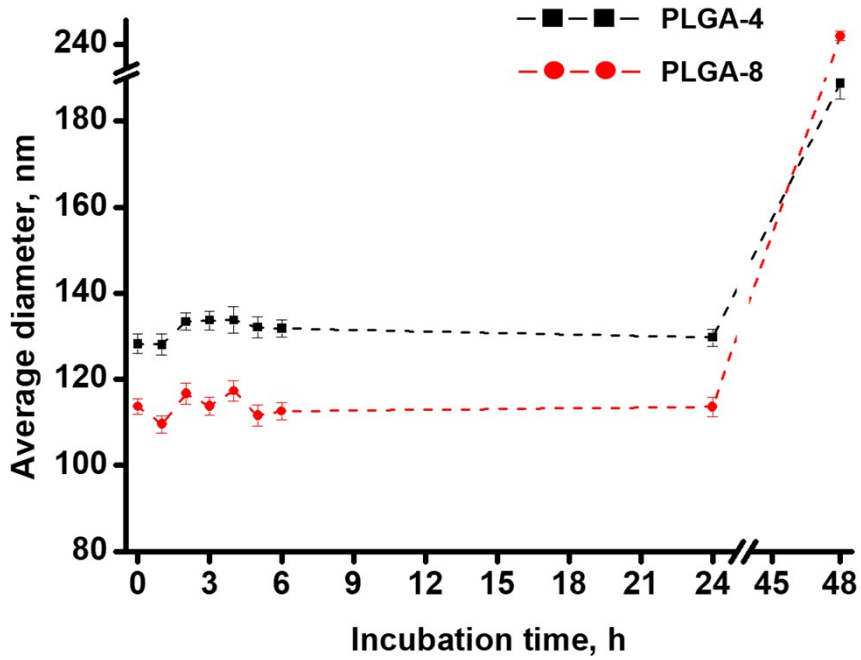

Figure S48. Dependence of the average size of nanoparticles (nm) from PLGA-**4** and PLGA-**8** polymers on time in experiments to study stability during incubation at 37 °C in RPMI-1640 media.

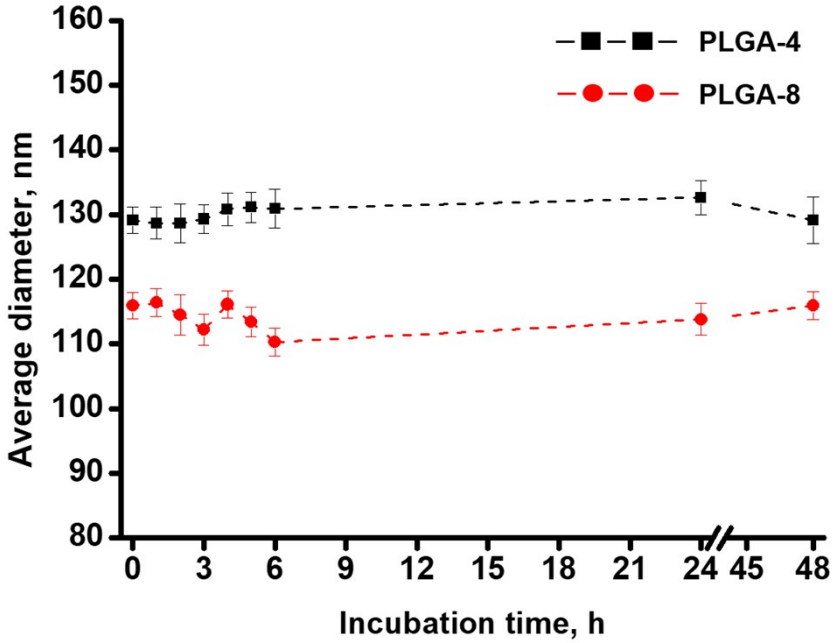

Figure S49. Dependence of the average size of nanoparticles (nm) from PLGA-**4** and PLGA-**8** polymers on time in experiments to study stability during incubation at 37 °C in DMEM media.

Table S6. Dependence of the average fluorescence intensity, relative to the initial value and expressed as a percentage, for nanoparticles made of PLGA-**4** and PLGA-**8** polymers, on time during incubation at 37 °C in PBS, RPMI-1640 and DMEM media

Time, h	PBS		RPMI-1640		DMEM	
	PLGA-4	PLGA-8	PLGA-4	PLGA-8	PLGA-4	PLGA-8
0,00	100,0±3,0	100,0±3,5	100,0±3,1	100,0±4,1	100,0±1,0	100,0±1,0
1,00	69,8±4,5	93,0±2,6	65,9±8,4	100,2±3,9	83,3±2,5	101,8±1,0
2,00	53,1±2,8	95,7±4,7	42,1±17,2	99,1±1,1	48,2±15,4	104,6±1,8
3,00	28,2±1,6	91,9±3,03	24,9±14,1	98,2±2,3	30,0±12,1	106,5±1,0
4,00	21,3±1,0	93,1±1,0	20,7±8,9	99,2±1,0	21,4±9,2	102,1±0,8
5,00	15,5±1,8	95,9±1,2	17,6±4,5	105,5±2,7	17,2±4,9	105,4±3,7
6,00	14,2±1,2	92,6±3,5	16,2±2,0	101,3±3,2	16,8±7,1	105,5±1,9
48,00	10,7±1,0	107,2±1,1	11,4±1,3	108,2±3,4	10,9±1,0	110,8±1,0

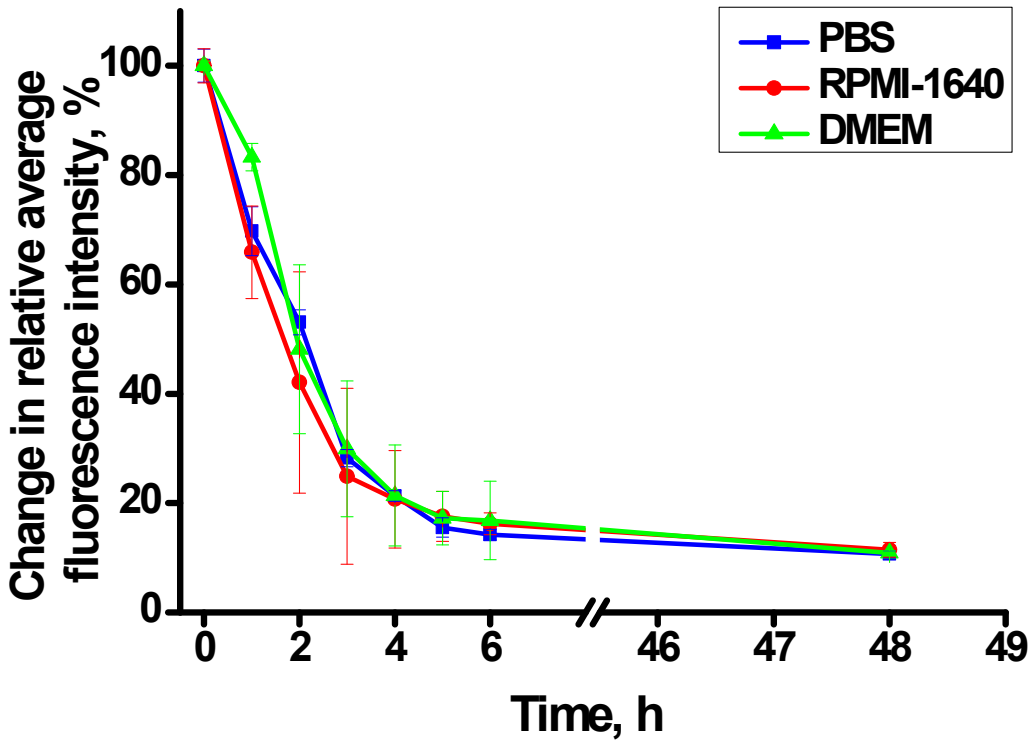

Figure S50. Dependence of the relative average fluorescence intensity of PLGA-**4** nanoparticles on time during incubation at 37 °C in PBS, RPMI-1640 and DMEM media

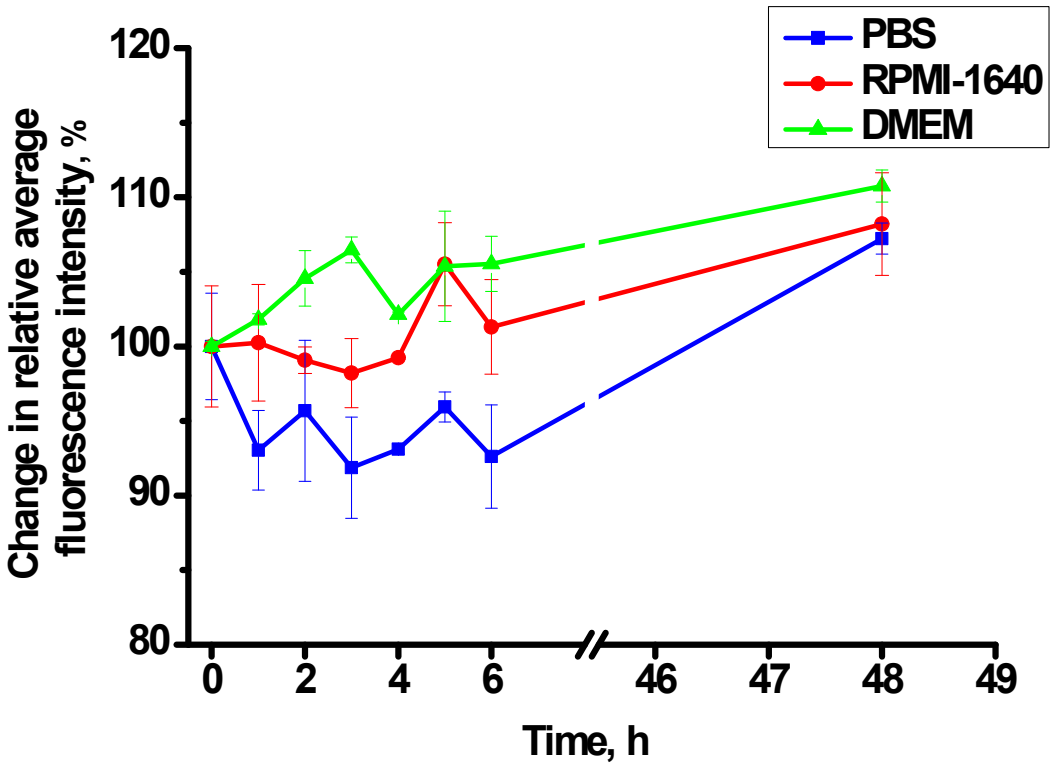

Figure S51. Dependence of the relative average fluorescence intensity of PLGA-**8** nanoparticles on time during incubation at 37 °C in PBS, RPMI-1640, and DMEM media

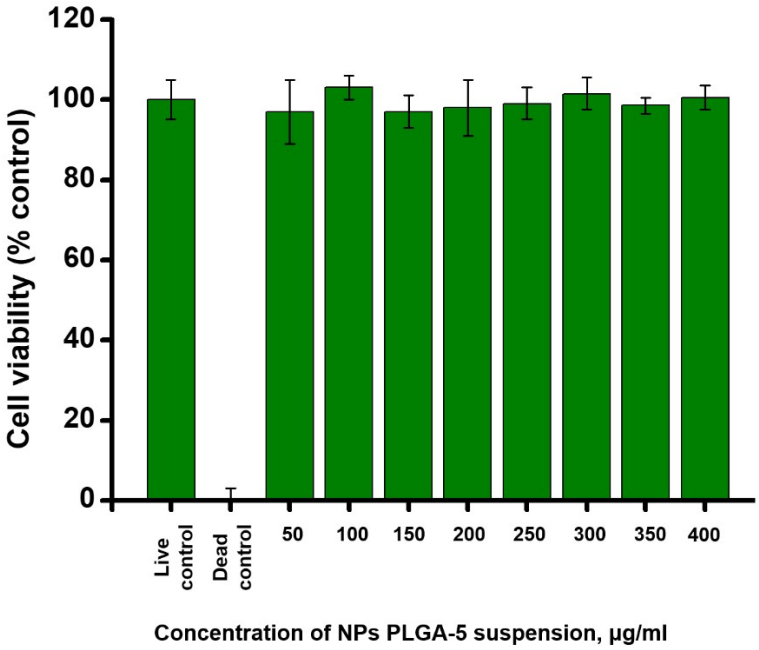

Figure S52. A study of the cytotoxicity of PLGA-**5** nanoparticles on the mouse breast carcinoma cell line 4T1 performed using a resazurin assay (Alamar Blue assay). Cell viability was assessed after 24-hour incubation. The experiment was performed in triplicate (n=3).

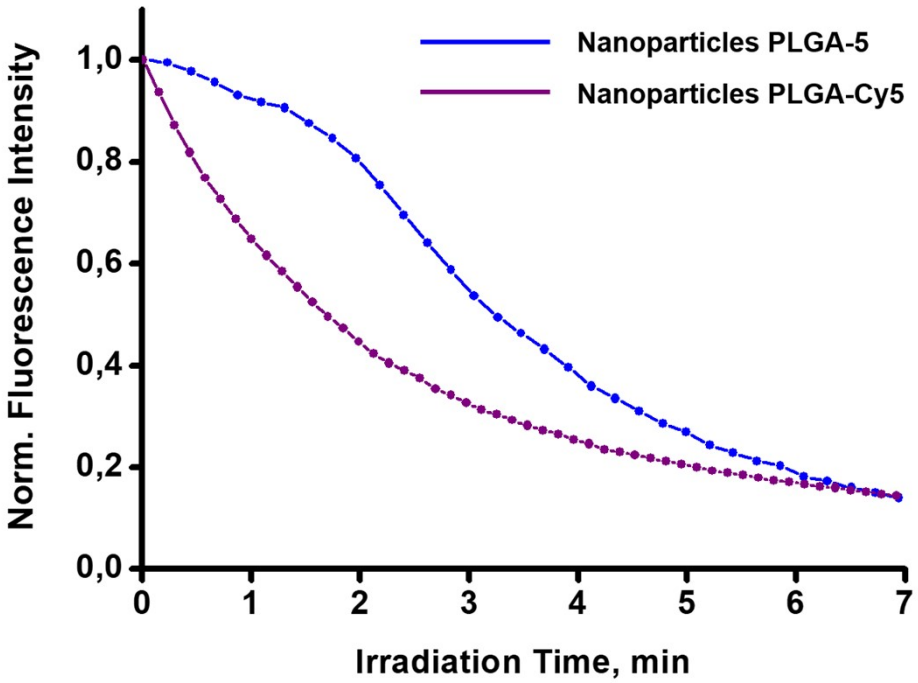

Figure S53. Time-dependent fluorescence intensity profiles of PLGA-naphthalimide 5 (blue) and PLGA-Cy5 (violet) nanoparticles following 7 min incubation. Selected regions of interest (ROI) were continuously bleached using 405 nm laser (PLGA-5) and 637 nm laser (PLGA-Cy5) over a 7 min irradiation period.

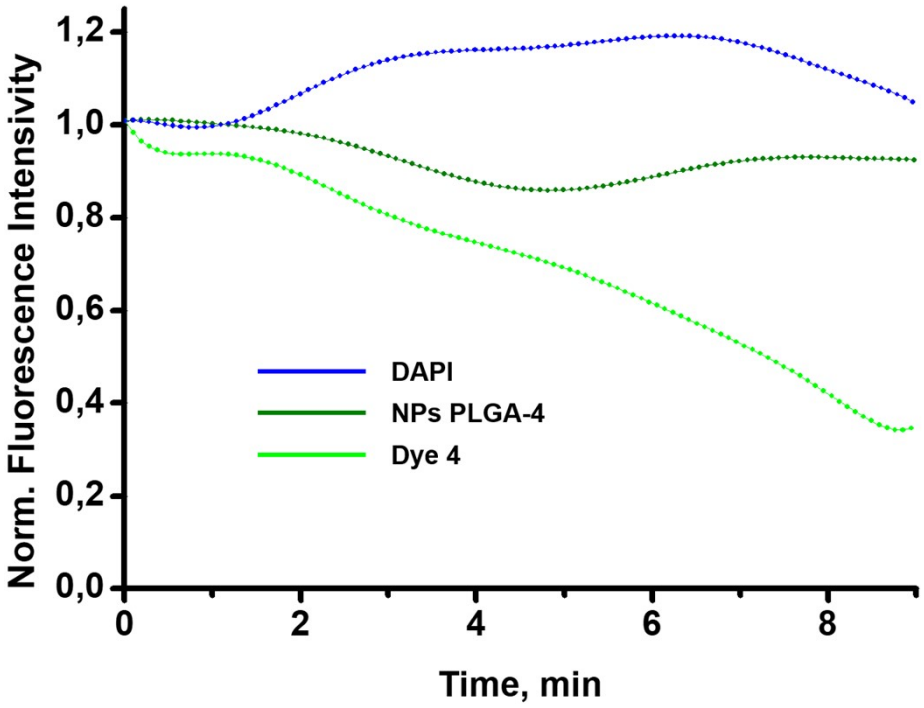

Figure S54. Time-dependent fluorescence intensity profiles of DAPI (blue) and PLGA-naphthalimide 4 nanoparticles(green) and dye 4 (light green) following 9 min incubation. Selected regions of interest (ROI) were continuously bleached using 405 nm laser over a 9 min irradiation period.

References

1. Choi S. *Yonsei Med. J.*, 2021, **62**, 11, 1042-1051.
2. Zhukova V. *Pharmaceutics*, 2021, **13**, 8, 1145.
3. Geng J. *Small*, 2013, **9**, 11, 2012-2019.
4. Liu M. *Pharmaceuticals (Basel)*, 2023, **16**, 6, 818-832.
5. Shahroosvand Z., Yeganeh N.R., Haddadian S. *Appl. Nanosci., 2020,* **10**, 1441–1452
6. Reul R. *Polym. Chem.*, 2012, **3**, 3, 694–702.
7. Czerney P. *Biol. Chem.*, 2001, **382**, 3, 495-498.
8. Kim J. S. J. *Colloid Interface Sci.*, 2011, **353**, 363-371.
9. Galliani M. *Chempluschem*., 2019, **84**, 11, 1653-1658.
10. Win K. W. *Small.*, 2015, **11**, 9, 1197-1204.